



This is a repository copy of *Directed evolution of biomass intensive CHO cells by adaptation to sub-physiological temperature*.

White Rose Research Online URL for this paper:

<https://eprints.whiterose.ac.uk/206367/>

Version: Published Version

Article:

Syddall, K.L., Fernandez–Martell, A., Cartwright, J.F. orcid.org/0000-0003-3132-6786 et al. (5 more authors) (2024) Directed evolution of biomass intensive CHO cells by adaptation to sub-physiological temperature. *Metabolic Engineering*, 81. pp. 53-69. ISSN 1096-7176

<https://doi.org/10.1016/j.ymben.2023.11.005>

Reuse

This article is distributed under the terms of the Creative Commons Attribution-NonCommercial-NoDerivs (CC BY-NC-ND) licence. This licence only allows you to download this work and share it with others as long as you credit the authors, but you can't change the article in any way or use it commercially. More information and the full terms of the licence here: <https://creativecommons.org/licenses/>

Takedown

If you consider content in White Rose Research Online to be in breach of UK law, please notify us by emailing eprints@whiterose.ac.uk including the URL of the record and the reason for the withdrawal request.



eprints@whiterose.ac.uk
<https://eprints.whiterose.ac.uk/>



Directed evolution of biomass intensive CHO cells by adaptation to sub-physiological temperature

Katie L. Syddall^a, Alejandro Fernandez-Martell^a, Joseph F. Cartwright^a,
Cristina N. Alexandru-Crivac^a, Adam Hodgson^b, Andrew J. Racher^{d,1}, Robert J. Young^c,
David C. James^{a,*}

^a Department of Chemical and Biological Engineering, University of Sheffield, Mappin St., Sheffield, S1 3JD, UK

^b Department of Molecular Biology and Biotechnology, University of Sheffield, Sheffield, S10 2TN, UK

^c Lonza Biologics plc, Cambridge, CB21 6GS, UK

^d Lonza Biologics Plc, Slough, SL1 4DX, UK

ARTICLE INFO

Keywords:

Recombinant therapeutics
Monoclonal antibody
CHO cells
Directed evolution
Metabolic engineering

ABSTRACT

We report a simple and effective means to increase the biosynthetic capacity of host CHO cells. Lonza proprietary CHOK1SV® cells were evolved by serial sub-culture for over 150 generations at 32 °C. During this period the specific proliferation rate of hypothermic cells gradually recovered to become comparable to that of cells routinely maintained at 37 °C. Cold-adapted cell populations exhibited (1) a significantly increased volume and biomass content (exemplified by total RNA and protein), (2) increased mitochondrial function, (3) an increased antioxidant capacity, (4) altered central metabolism, (5) increased transient and stable productivity of a model IgG4 monoclonal antibody and Fc-fusion protein, and (6) unaffected recombinant protein N-glycan processing. This phenotypic transformation was associated with significant genome-scale changes in both karyotype and the relative abundance of thousands of cellular mRNAs across numerous functional groups. Taken together, these observations provide evidence of coordinated cellular adaptations to sub-physiological temperature. These data reveal the extreme genomic/functional plasticity of CHO cells, and that directed evolution is a viable genome-scale cell engineering strategy that can be exploited to create host cells with an increased cellular capacity for recombinant protein production.

1. Introduction

Chinese Hamster Ovary (CHO) cells demonstrate remarkable phenotypic plasticity, being able to adapt to the wide range of industrial processes required to meet the demands of modern biopharmaceutical manufacturing (Costa et al., 2011; Sinacore et al., 2000; Dahodwala and Lee, 2019). Industrial CHO cell lines are inherently “fit-for-purpose”, exhibiting a high capacity for cell and product biomass synthesis and robust cell culture process performance. Whilst these attributes have been improved via genetic engineering, cell culture process control or media optimisation (McVey et al., 2016; Budge et al., 2020; Handlogten et al., 2018; Pan et al., 2017), they have also been derived by adaptive evolution (e.g., to suspension growth in chemically defined media) and directed selection of clonal variants. Such methods effectively harness CHO cell genetic/functional heterogeneity by enriching the existence of

desirable traits (Sinacore et al., 2000; Prentice et al., 2007; Sunley et al., 2008; Bort et al., 2010; Costa et al., 2011; Fernandez-Martell et al., 2018; Chandrawanshi et al., 2020; Weinguny et al., 2020; Mistry et al., 2021; Chakrabarti et al., 2022).

With respect to cell culture process optimisation, relatively simple and robust manipulations have typically had the most positive impact on key fed-batch process metrics such as volumetric titre and cell viability. For example, to mitigate the decline of cellular biosynthetic capacity during culture, many industrial manufacturing processes implement the concept of biphasic cultivation, wherein an initial rapid cell proliferation phase is achieved by cultivating cells at physiological temperature (i.e. 37 °C), followed by a cell proliferation arrest phase resulting from a shift to low cultivation temperature (i.e. 28–33 °C) to ensure maximal protein production (Yoon et al., 2004; Gomes and Hiller, 2018). Although improved culture performance has been achieved by

* Corresponding author.

E-mail address: d.c.james@sheffield.ac.uk (D.C. James).

¹ Current address: HigherSteaks Ltd, Unit 2, TechnoPark, Cambridge CB5 8 PB, UK.

implementing biphasic cultivation (Ahn et al., 2008; Al-Fageeh et al., 2006; Fox et al., 2004; Xu et al., 2019), the intrinsic cell cycle arrest imposes a limit on the viable cell concentration (VCC) from this point onwards. To overcome this inherent drawback, attempts to adapt stably producing cell lines to hypothermic conditions have been made. However, this has generally not resulted in any wholly successful outcomes for recombinant protein production due to reduced specific productivities or cells becoming fragile as they were re-adapted to suspension culture (Sunley et al., 2008; Yoon et al., 2006).

In this study we subjected non-producing host CHOK1SV® cells to hypothermic conditions (32 °C) for over 150 generations to create evolved CHO variants with recovered proliferation rates, relative to the proliferation rates of their progenitor parental populations when cultured at 37 °C. Evolved cells also had an increased average cell volume (1.7-fold), and increased (2-fold) cellular biomass content (total RNA and protein). Additionally, evolved cells exhibited significantly increased transient and stable production of recombinant proteins (IgG4 mAb and an Fc-fusion protein) without negative impacts upon N-glycan processing. Moreover, our data indicate that this phenotypic transformation of host CHO cells to an inherently more biomass intensive and productive state was facilitated by enhanced oxidative metabolism, a reduced cellular content of reactive oxygen species (ROS), and differential utilisation of carbon source, amino acid and fatty acid metabolism. These changes were underpinned by extensive karyotype and gene expression changes, the scale of which would be difficult to achieve with current genetic engineering technologies. Overall, we demonstrate a very simple and effective means to significantly increase the synthetic capacity of host CHO cells using a facile culture process manipulation as a selective pressure.

2. Materials and methods

2.1. CHO cell culture

A host CHOK1SV® cell line was provided by Lonza Biologics (Slough, UK). Routine cell culture (hereafter referred to as standard conditions) was carried out in 125 mL vented Erlenmeyer flasks (Corning, Surrey, UK) at a working volume of 30 mL in CD-CHO medium containing 6 mM L-glutamine (Thermo Fisher Scientific, Loughborough, UK). Cells were sub-cultured according to a 3-4 d regime at a seeding concentration of 2×10^5 viable cells mL⁻¹ and maintained at 37 °C, 140 rpm and 5% CO₂, unless otherwise stated. Stable pools were similarly maintained but used CD-CHO medium supplemented with 25 µM methionine sulfoximine (MSX) and without L-glutamine. VCC, cell viability and average cell diameter was routinely measured using a Vi-CELL XR (Beckman Coulter, High Wycombe, UK). Average cell volume was calculated as follows:

$$v [mm^3] = \left(\frac{4}{3}\right) \pi r^3 \quad (1)$$

Where v is the average cell volume and r is the average cell radius. The time integral of viable cell concentration (IVCC) and the time integral of viable cell volume (IVCV) were calculated as follows:

$$IVCC [cell hml^{-1}] = \frac{(x_1 - x_0)(t_1 - t_0)}{\ln\left(\frac{x_1}{x_0}\right)} \quad (2)$$

$$IVCV [mm^3 hml^{-1}] = \frac{(v_1 x_1 - v_0 x_0)(t_1 - t_0)}{\ln\left(\frac{x_1}{x_0}\right)} \quad (3)$$

Where x_1 and x_0 are the VCC at final and initial timepoints, respectively, t_1 and t_0 are the time at final and initial time points, respectively, and v_1 and v_0 are the average cell volume at final and initial time points, respectively. Based upon previous studies (Dungrawala et al., 2010; Padovan-Merhar et al., 2015; Zhurinsky et al., 2010; Marguerat and

Baehler, 2012) we assume a linear relationship between cell volume and biomass accumulation, and a positive correlation between cell size and productivity (Schellenberg et al., 2022). Therefore, we choose to primarily use IVCV over IVCC, because we believe it is a more accurate representation of cell biomass accumulation during cell culture and is more useful when considering the relationship between biomass accumulation and productivity, especially given the variation in cell volume between populations.

2.2. Hypothermic cell culture

Three independent CHOK1SV® cell cultures (termed parental cells; P-A, P-B and P-C) were each used to seed two Erlenmeyer flasks at a concentration of 1×10^6 viable cells mL⁻¹, which were maintained in either standard conditions (control cultures) or hypothermic conditions (32 °C, 5% CO₂, 140 rpm – evolved cultures) for over 150 generations. Due to initial slow proliferation rates, evolved cultures were sub-cultured at a seeding concentration of 1×10^6 viable cells mL⁻¹ every 7 d for the first 8 passages and once proliferation rates had recovered cells were sub-cultured according to a 3-4 d regime at 2×10^5 viable cells mL⁻¹. Control cultures were sub-cultured according to a 3-4 d regime at 2×10^5 viable cells mL⁻¹ throughout. After over 150 generations, three independent control cell populations growing at 37°C (termed control cells; 37A, 37B, and 37C) and three independent evolved cell populations growing at 32°C (termed evolved cells; 32A, 32B, and 32C) were established.

2.3. Total cellular RNA content quantification

Mid-exponential growth phase cells were centrifuged (200×g, 5 min) and 5×10^6 cells were taken from each culture for RNA extraction and quantification using a RNeasy® Mini Kit (QIAGEN, Manchester, UK) according to the manufacturer's instructions. RNA concentrations were measured using a Nanodrop™ 2000 Spectrophotometer (Thermo Fisher Scientific).

2.4. Total cellular protein content quantification

Mid-exponential growth phase cells were centrifuged (200×g, 5 min) and washed twice in phosphate buffered saline (PBS; Sigma-Aldrich, Poole, UK). Cells (5×10^6) were lysed in 1 mL RIPA buffer (Thermo Fisher Scientific) supplemented with Protease Inhibitor cocktail (Thermo Fisher Scientific) according to the manufacturer's instructions. Protein concentration was determined using a Pierce BCA protein assay kit (Thermo Fisher Scientific) according to the manufacturer's instructions. Optical density was measured (562 nm) using a PowerWave XS™ microplate reader (BioTek, Potton, UK).

2.5. Measurement of cellular reactive oxygen species (ROS)

CellROX® Deep Red Reagent (Thermo Fisher Scientific) was added to 2 mL of mid-exponential cells at a final concentration of 5 µM and incubated at ambient room temperature (RT) for 30 min. Unstained control samples were also incubated for the same duration. Cells were then centrifuged (200×g, 5 min) and washed twice with PBS before fixing with 4% (v/v) PFA. Fixed samples were analysed using a BD LSRII Flow Cytometer (BD Biosciences, Oxford, UK) using the Red 660 nm laser configuration.

2.6. Karyotyping and G-Banding

Chromosome spreads and G-Banding were prepared as follows: Mid-exponential phase cells (1×10^6) were treated with KaryoMAX™ Colcemid Solution (Thermo Fisher Scientific, 0.08 µg mL⁻¹) for 3h at 37 °C and 32 °C for P-A and 32A cell populations, respectively. Cells were centrifuged (270×g, 8 min) and resuspended in a hypotonic solution (50

mM KCl) for 8 min at RT. Cells were fixed by dropwise addition of fixative (3:1 methanol:acetic acid). Metaphase spreads were prepared by air-drying a 40 μ L droplet of fixed cells onto an ice-cold microscope slide. Slides were aged for 2 days at RT, partially digested with Trypsin (Thermo Fisher Scientific, 1:250) for 10s, and washed in Sorensen's buffer. Slides were rinsed and stained in Leishman's stain: Gurr Buffer (Thermo Fisher Scientific, 1:4), washed in Gurr buffer, and then mounted using DPX (Sigma-Aldrich) and a 20 \times 50 mm coverslip. Metaphase spreads were analysed at 100X using an Olympus BX51 microscope.

2.7. Flow cytometric ploidy analysis

Mid-exponential growth phase cells (1×10^6) were centrifuged (200 \times g, 5 min), fixed using 4% (v/v) PFA, washed with PBS, centrifuged (200 \times g, 5 min), stained with 0.5 mL of FxCycle™ PI/RNase Staining Solution (Thermo Fisher Scientific) and incubated for 30 min at RT. Cells were analysed on a BD LSRII Flow Cytometer (BD Biosciences) using 532 nm excitation and emission collected with a 585/42 bandpass filter.

2.8. Metabolite quantification

Glucose and lactate concentrations were determined using a Cedex Bio analyser (Roche Diagnostics Ltd., West Sussex, UK) according to manufacturer instructions. Essential amino acid (EAA) and non-essential amino acid (NEAA) concentrations were determined by AltaBioscience laboratories (Birmingham, UK): Briefly, samples were mixed 1:1 with 5% (v/v) TCA and centrifuged (10,000 rpm, 5 min) to precipitate protein. The resulting solution (25 μ L) was injected into a Biochrom amino acid analyser (Cambridge, UK) with a lithium buffer system and post-column ninhydrin derivatisation. Duplicate metabolic analyses were performed using pre- and post-feeding samples of cell-free supernatant from days 0, 3, 6, and 9 of fed-batch culture (FBC). To exclude cell volume effects, cell-specific metabolic rates (qMet) were corrected using the IVCV.

2.9. Analysis of mitochondrial bioenergetics

The oxygen consumption rate (OCR) of intact cells was measured using a cell metabolic analyser Seahorse XF24 (Seahorse Biosciences, North Billerica, MA) as described in Fernandez-Martell et al. (2018). OCR measurements of control and evolved cells were performed at 37 °C and 32 °C, respectively, with final concentrations of 1.5 μ M Oligomycin, 0.75 μ M FCCP and 1 μ M Antimycin A/Rotenone. XF24 operating temperature (i.e., 37 °C or 32 °C) did not significantly influence OCR. To exclude any cell plating effects, OCR data was normalized by cell number (CyQUANT Cell proliferation kit – Thermo Fisher Scientific) and corrected using the IVCV. Derivative mitochondrial functions (basal respiration, ATP turnover, proton leak, maximal respiration, spare respiratory capacity, coupling efficiency, and non-mitochondrial respiration) were calculated according to Brand and Nicholls (2011) by combining the sequential effects of optimised concentrations of oligomycin (ATP synthase inhibitor), FCCP (electron transport chain accelerator) and rotenone plus antimycin A (ETC inhibitors), as previously described in Fernandez-Martell et al. (2018).

2.10. Plasmid DNA preparation

Plasmids encoding IgG4 mAb and Fc-fusion protein were supplied by Lonza Biologics. Transformed *E. coli* cultures were expanded, and plasmid DNA was purified using the QIAGEN Plasmid Plus Giga kit (QIAGEN) according to the manufacturer's instructions.

2.11. Transient fed-batch production by lipofection

Cell aliquots (10 mL, VCC: $\sim 1.0 \times 10^6$ cells mL⁻¹) were dispensed

into 50 mL TubeSpin bioreactor tubes (TPP, Trasadingen, Switzerland) and transfected using Lipofectamine® LTX with PLUS™ (Thermo Fisher Scientific). DNA–Lipofectamine LTX (1:2) complexes were prepared according to manufacturer instructions with a total DNA load of 12 μ g (per aliquot), incubated at room temperature for 5 min and then added to cells. 37A and 32A cell cultures were incubated (170 rpm, 5% CO₂) at 37°C and 32°C, respectively, for 12 d with a feeding regimen of 10% (v/v) EfficientFeed™ B (Thermo Fisher Scientific) on days 3, 6 and 9 post-transfection.

2.12. Generation of stable pools

Mid-exponential phase cells were centrifuged (200 \times g, 5 min), resuspended in CD CHO media (VCC: 14.3×10^6 cells mL⁻¹) and transferred (700 μ L) to a 0.4 cm electroporation cuvette (Bio-Rad, Hemel Hempstead, UK) containing 40 μ g linearised DNA in 100 μ L TE buffer. Cells were electroporated (300 V, 900 μ F, ∞ Ω) using a Gene-Pulser Xcell™ (Bio-Rad), transferred to a T175 cm flask (Thermo Fisher Scientific) containing 50 mL warmed CM55 media (Lonza Biologics), and incubated (10% CO₂, 85% humidity) at 37°C or 32°C for 37A and 32A cells, respectively. After 24h, 50 mL of selection media (CM55 + 100 μ M MSX) was added to give a final MSX concentration of 50 μ M. After cell viability recovery, stable pools were maintained in 125 mL vented Erlenmeyer flasks with 25 μ M MSX.

2.13. Quantification of IgG4 mAb and Fc-fusion recombinant proteins

IgG4 mAb and Fc-fusion protein titres were measured using a FastELISA® Human IgG Quantification kit (RD-Biotech, Besançon, France), according to the manufacturer's instructions. Optical absorbance of each sample was measured at 450 nm using a PowerWave XS™ microplate reader.

2.14. Purification of IgG4 mAb and Fc-fusion recombinant proteins

Recombinant IgG4 mAb and Fc-fusion protein were purified using HiTrap Protein A prepacked columns (GE Healthcare, Buckinghamshire, UK) according to manufacturer instructions. Purified protein concentration was measured at 280 nm using a NanoDrop™ 2000 Spectrophotometer. Protein was stored in PBS at -20°C before further analysis of glycan profiles.

2.15. N-glycan analysis

IgG4 mAb and Fc-fusion N-glycans were purified using a ProZyme GlycoPrep system (ProZyme, CA, USA) according to the manufacturer's instructions: Briefly, under denaturing conditions, purified protein was deglycosylated by peptide-N-glycosidase F (PNGaseF) digestion. N-linked oligosaccharides were dried in a centrifugal vacuum evaporator (SpeedVac) and labelled with 2-aminobenzamide fluorophore (2-AB). Non-glycan contaminants were removed using a GlykoPrep® resin (Agilent, CA, USA) and organic solvent washes. Captured glycans were eluted in HPLC water. Glycan analysis was performed by hydrophilic interaction chromatography (HILIC) on a Waters UPLC controlled by Empower 2 using a Waters BEH Glycan column (Waters, Hertfordshire, UK).

2.16. RNA sequencing analysis

Cell pellets from populations 32A and 37A were collected in triplicate on day 3 of FBC and sent to Affymetrix (CA, USA) for RNA sequencing at a minimum depth of 30 million single-end reads. Quality control of raw reads was performed using FastQC (<https://www.bioinformatics.babraham.ac.uk/projects/fastqc/>), followed by alignment to the CHO genome (GCF_003668045.3_CriGri-PICRH-1.0) with STAR (Dobin et al., 2013) using default parameters and gene-level quantification with

FeatureCounts (Liao et al., 2014). Raw counts were then filtered for genes with no expression in all samples and differential expression analysis was performed using DESeq2 (Love et al., 2014). Variance stabilizing transformation (VST) was applied to the normalized counts, prior to PCA visualization. The significance threshold was $\text{Padj} < 0.05$ and results were sorted by $\log_2\text{FoldChange}$. Orthologous analysis was performed through a forward and reverse “all-vs-all BLASTp” (BLAST® Command Line Applications User Manual) between the CHO (PICRH) and mouse (GRCm39) genomes. Mouse orthologous names and Entrez IDs were used for the downstream GO terms (Ashburner et al., 2000; Carbon et al., 2021) and KEGG pathway (Kanehisa and Goto, 2000; Kanehisa et al., 2022) analyses. The *ontologyIndex* (Greene et al., 2017) and *pathview* (Luo and Brouwer, 2013) R libraries were used to download the full GO ontology and KEGG pathways found in mouse (mmu). Gene names (symbols), Entrez IDs and their corresponding GO IDs were retrieved from the mouse Bioconductor annotation database (org.Mm.eg.db) via AnnotationDbi. These were then filtered for mouse

orthologues of genes expressed in our dataset and linked to GO terms and KEGG pathways.

3. Results

3.1. Hypothermic adaptation yields larger CHO cells with a recovered proliferation rate

Hypothermic conditions typically induce cell cycle arrest at G1 phase (Moore et al., 1997), so we hypothesised that long-term hypothermic culture would select for CHO cell variants with an increased capability to proliferate under this constraint. Three independent CHOK1SV® cell cultures (termed parental; P-A, P-B, and P-C) were routinely cultured for over 150 generations at both 37 °C or 32 °C (standard or hypothermic conditions) to establish control (37A, 37B, and 37C) and evolved (32A, 32B, and 32C) cell populations, respectively. All populations had a cell viability >95% (data not shown). Over this period the average

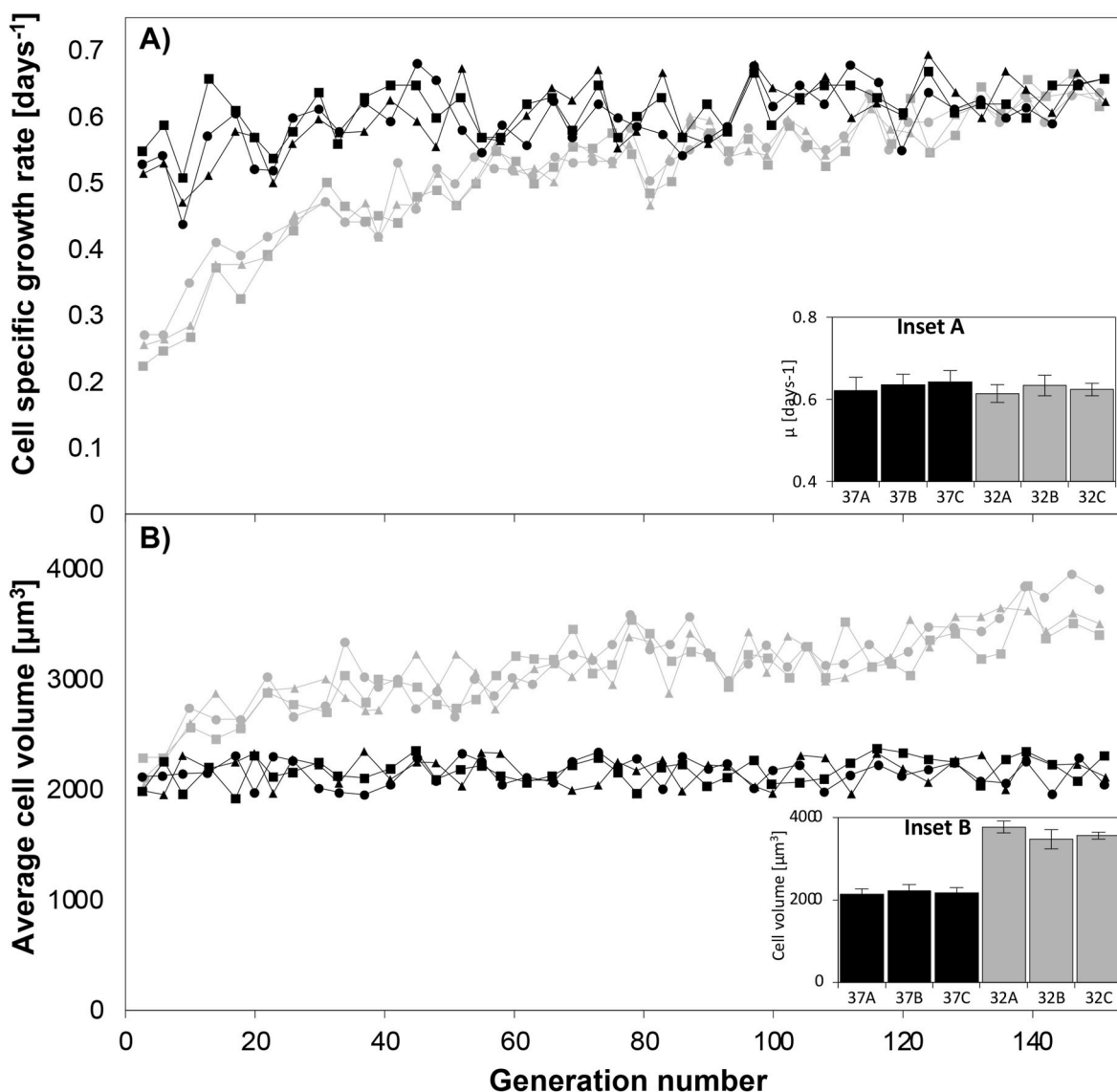


Fig. 1. Effect of long-term mid-hypothermic evolution on CHO cell proliferation and average cell volume. Three parental cultures of CHOK1SV cells were divided into duplicate culture flasks. For each duplicate, one flask was continuously sub-cultured at 37 °C (control) and the second flask at 32 °C (evolved) for 150 over generations to establish control (37A, 37B, and 37C) and evolved (32A, 32B, and 32C) cell populations, respectively. Specific cell proliferation rate (A) and average cell volume (B) were measured approximately every 3–4 days throughout this process ($n = 1$). Black and grey lines represent the control and evolved populations, respectively. For both control and evolved populations lineages A, B and C are shown using circles, squares, and triangles, respectively. The inset bar charts show the mean specific cell proliferation rates (inset A) and average cell volumes (inset B) of each population at the end of the cell culture regime ($n = 3$). Black and grey bars represent the control and evolved populations, respectively.

proliferation rate of evolved cells maintained at 32 °C gradually recovered, from 0.25 days⁻¹ to 0.63 days⁻¹ (Fig. 1A), approximately equalling the proliferation rate of control cells maintained at 37 °C. Evolved cells also significantly ($p < 0.002$) increased in average cell volume, from 2143 μm^3 to 3577 μm^3 (1.7-fold; Fig. 1B). Control cell proliferation rate did increase marginally, from an average of 0.53 days⁻¹ to 0.65 days⁻¹, which is in line with previous reports of increased proliferation rates over long-term culture (Davies et al., 2013). Control cells showed no significant changes in average cell volume (Fig. 1B) and remained otherwise phenotypically similar to the original parental cell populations (data not shown). A summary of growth, karyotype, and biomass phenotypes of parental, control and evolved cells (where measured) can be found in Table 1. Adaptation to more extreme hypothermia (30 °C) was attempted in which cells remained viable but did not recover proliferation rate (data not shown).

3.2. Hypothermic adaptation yields CHO cells with increased biomass content and genomic heterogeneity

Previous findings that have shown that global transcription rates (Dungrawala et al., 2010; Padovan-Merhar et al., 2015; Zhurinsky et al., 2010) and protein content (Marguerat and Baehler, 2012) scale with cell volume. To determine whether the increase in cell volume during adaptation to 32 °C was associated with a corresponding increase in cellular biomass, we measured the total RNA and protein content of mid-exponential phase cells cultured at 37 °C and 32 °C (Fig. 2A and B). Cells evolved for growth at 32 °C showed a significant increase in total RNA (~1.81-fold; $p < 0.02$) and protein (~1.66-fold; $p < 0.02$) content compared to cells continuously grown at 37 °C. Whilst this likely demonstrates that biomass synthesis scales with cell volume, it might also be the case that culturing cells at 32 °C increases the half-life of cellular components, thus reducing the rate of turnover and increasing cellular biomass.

An increase in mammalian cell size often correlates with an increase in DNA content through the mechanism of DNA endoreplication to maintain higher levels of protein synthesis for maintenance of larger cells (Gillooly et al., 2015; Lee et al., 2009). To ascertain whether there had been any changes to chromosomal DNA as a result of adaptation to 32 °C, we compared the overall DNA content and karyotype of mid-exponential phase cells from population 32A with that of its progenitor parental population, P-A. Overall DNA content, measured by flow cytometry (Fig. 2C; Table 1), was approximately the same within cells from both populations, suggesting that total DNA content did not increase with cell volume. However, our analysis did reveal differences in cell cycle progression. The increase in G1/G0 phase cells and reduction in G2/M phase cells within the 32A population indicates an extended G1 phase and a relatively quicker transition of cells through G2 and M phases, seemingly allowing cells to accumulate more cell mass without compromising the rate of cell division (Ginzberg et al., 2015).

Table 1
Parental, Control, and Evolved cell phenotypes.

		Cell Volume (μm^3) ^a	Cell Diameter (μm) ^a	Cell Specific Growth Rate (days ⁻¹) ^a	Chromosome Number ^a	DNA content (DI) ^b	RNA Biomass (pg cell ⁻¹) ^a	Protein Biomass (pg cell ⁻¹) ^a
Parental	P-A	2111.7	15.94	0.529	19	1.46	4.24	169.5
	P-B	2140.8	15.60	0.548	-	-	4.56	200
	P-C	2009.74	15.60	0.515	-	-	4.70	189.5
Control	37A	2129.6	15.76	0.622	-	-	-	-
	37B	2230.4	16.34	0.636	-	-	-	-
	37C	2178.0	15.92	0.642	-	-	-	-
Evolved	32A	3773.9	19.39	0.614	33	1.345	8.77	324.2
	32B	3477.7	18.67	0.634	-	-	7.76	296.8
	32C	3565.8	18.85	0.624	-	-	7.86	309.5

- Not measured.

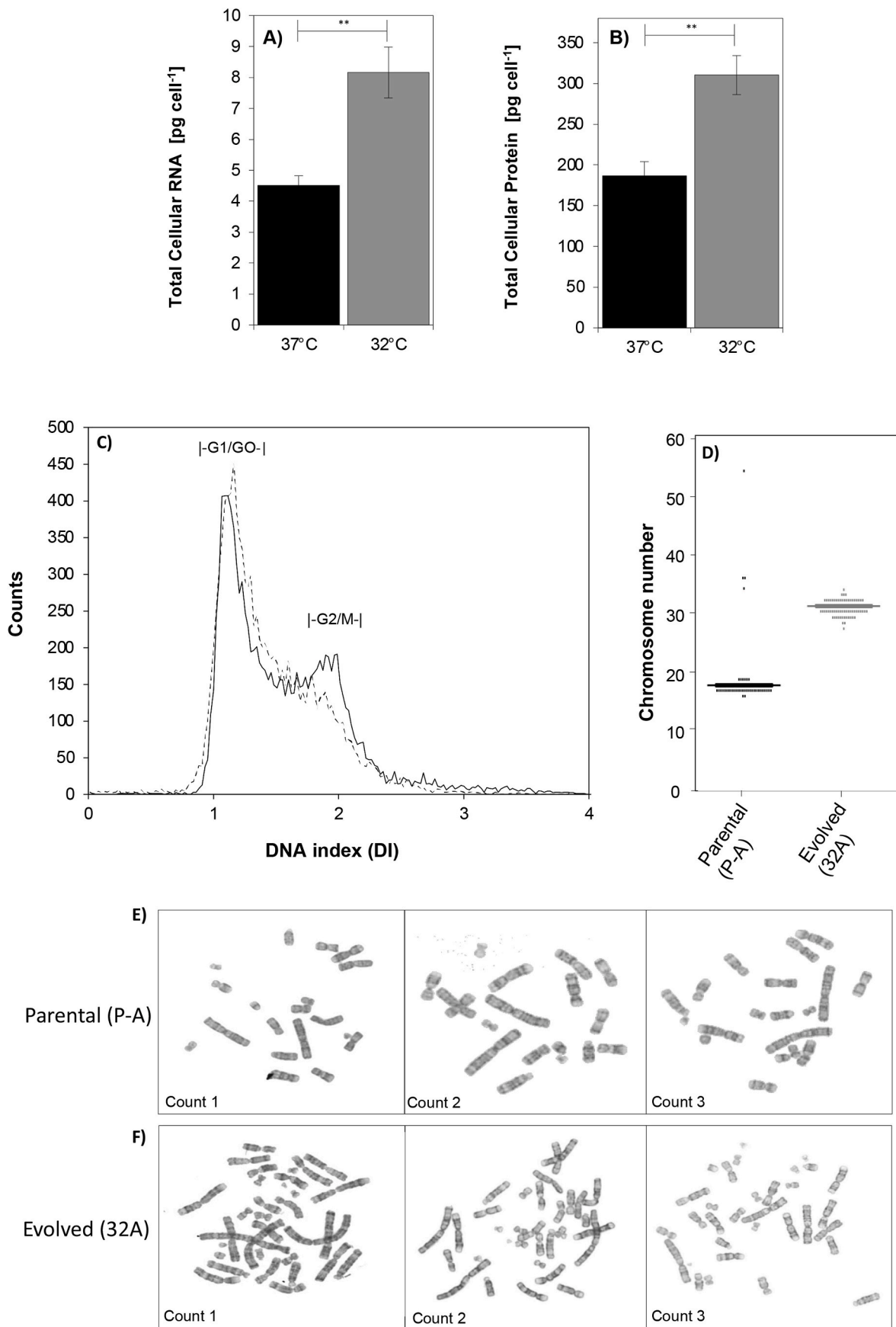
^a Average.

^b Median.

The broader peak relating to G0/G1 phase cells suggests the presence of chromosomal variation (aneuploidy) in both populations and the less prominent G2/M peak for 32A cells demonstrates a potential lack in cell cycle checkpoint fidelity. In accordance with this, analysis of metaphase spreads showed increased mean chromosome numbers per cell (Fig. 2D) in 32A cells (~33 chromosomes) compared to P-A cells (~19 chromosomes) and that these differences were observed as both whole chromosome and segmental aneuploidy (Fig. 2E and F). Taken together these data indicate that the increase in evolved cell chromosome number, despite an unchanged DNA content, resulted from chromosomal rearrangement and minor deletions or duplications, rather than gross changes in ploidy (i.e., endoreplication). We therefore infer that the CHOK1SV® population (or sub-populations within) are prone to aneuploidy (or defective mitotic checkpoints) with elevated levels of chromosomal instability which could result from, or be potentiated by, a loss of cell cycle checkpoint fidelity. Chromosomal aberrations are often proposed to facilitate adaptation (Duncan et al., 2012; Sansregret and Swanton, 2017; Yoon et al., 2002), and so perhaps genomic change may have been a primary mechanism for phenotypic adaptation of evolved cells (e.g., increased cellular biomass) under hypothermic conditions.

3.3. CHO cell adaptation to hypothermia is associated with elevated mitochondrial activity

We have demonstrated considerable phenotypic similarity between the replicate control populations (37A, 37B, and 37C) and between the replicate evolved populations (32A, 32B, and 32C) cell populations. Therefore, it was decided to proceed only with comparisons between 32A and 37A for all subsequent analyses, which are comparatively resource intensive. Mitochondria are central to energy and biosynthetic precursor generation, cellular redox (linked to DNA damage), and thermogenesis (Templeton et al., 2013; Young, 2013; Das Neves et al., 2010; Fedorenko et al., 2012). We hypothesised that the ability of evolved cells to increase cellular biomass and proliferation rate at 32 °C would require an altered mitochondrial activity and oxidative metabolism. Mitochondrial function of mid-exponential 37A and 32A cell populations was analysed using microplate-based measurement of oxygen consumption rate (OCR) to determine the following derivative mitochondrial functions: basal respiration, ATP turnover, proton leak, maximal respiration, spare respiratory capacity, coupling efficiency, and non-mitochondrial respiration (Fig. 3A). 32A cells exhibited a significant increase in mitochondrial function (basal oxygen consumption: 1.76-fold, $p < 0.01$; ATP turnover: 1.83-fold, $p < 0.001$; maximal respiration: 1.53-fold, $p < 0.05$; proton leak: 1.52-fold, $p < 0.05$; non-mitochondrial respiration: 1.45-fold, $p < 0.01$; Fig. 3A) compared to 37A cells. However, spare respiratory capacity (ability of electron transport to satisfactorily respond to an increase in energy demand under intense physiological stimulus) and mitochondrial coupling efficiency (78.9–81.8%; the fraction of basal oxygen consumption used for



(caption on next page)

Fig. 2. Analysis of Biomass content, DNA content and karyotype within CHOK1SV cells evolved to 32 °C. Total RNA (A) and protein (B) content of the evolved cell populations (grey) is presented in comparison with cells cultured routinely at 37 °C (black). Each cell population was measured in triplicate and statistical significance was calculated by Student's t-test and is indicated as follows: * $P < 0.05$, ** $P < 0.01$, *** $P < 0.001$. C) Mid-exponential 32A and P-A cells were harvested for flow cytometric analysis of DNA content using FxCycle™ PI/RNase Staining Solution. The solid and dashed lines represent P-A and 32A populations, respectively, and both represent the analysis of >11,000 cells. D) Metaphase spreads were prepared to analyse the number of chromosomes present in populations P-A ($n = 126$; black) and 32A ($n = 111$; grey). Three example metaphase spreads are presented from populations P-A (E) and 32A (F) to demonstrate the difference in chromosomal structure between the two populations.

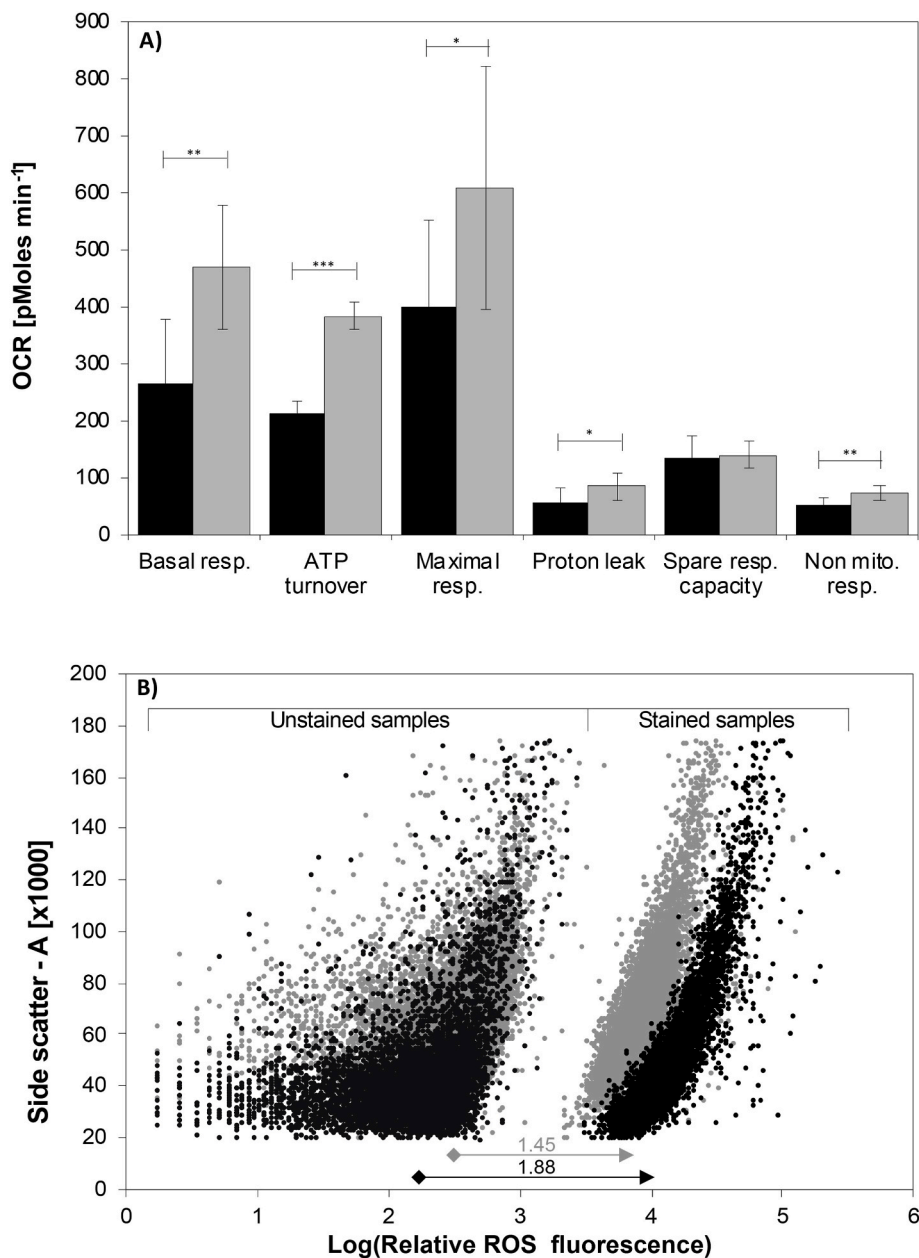


Fig. 3. Quantitative dissection of mitochondrial bioenergetics and cytosolic ROS activity. **A)** Measurements of OCR were performed on populations 37A and 32A at temperatures native to cell type (control 37A – 37 °C; evolved 32A – 32 °C) in un-buffered DMEM and after injection of each of the following compounds: oligomycin, FCCP and rotenone plus antimycin A. OCR data was normalized by cell number and corrected using the IVCV to present data as a function of cellular biomass. The following mitochondrial functions were derived: Basal mitochondrial respiration, ATP turnover, maximal respiration, spare respiratory capacity, proton leak, non-mitochondrial respiration, and coupling efficiency of 37A (black) and 32A (grey) cell populations. Statistical significance ($n = 3$) was calculated by Student's t-test and is indicated as follows: * $P < 0.05$, ** $P < 0.01$, *** $P < 0.001$. **B)** Cytosolic ROS activity was quantified by flow cytometry ($n > 10,000$ cells) three days post-subculture in populations 37A (black) and 32A (grey) using CellROX® Deep Red Reagent.

ATP synthesis) were unchanged, meaning that these important survival mechanisms were not compromised during the evolution process (Desler et al., 2012).

The majority of endogenous ROS are generated in mitochondria

(Balaban et al., 2005; Rial and Zardoya, 2009), so to assess whether intracellular levels of oxidative stress scaled with mitochondrial functions we measured the oxidative status of 37A and 32A cell populations in complete growth media using flow cytometry. 32A cells had lower

levels of intracellular ROS compared to 37A cells (Fig. 3B), suggesting that evolved cells have an enhanced antioxidant resilience.

Overall, these data indicate that an increased mitochondrial capacity was necessary to meet the metabolic requirements of the larger, biomass-intensive and proliferative evolved cells at 32 °C, which was achieved whilst decreasing intracellular ROS. Furthermore, increases in proton leakage (indicative of oxygen consumption that is not coupled to ATP production) and ROS mitigation are fundamental features of adaptive non-shivering thermogenesis (Fedorenko et al., 2012;

Klingenspor et al., 2008), an adaptive mechanism by which evolved cells could have generated metabolic heat in response to culture at 32 °C.

3.4. Metabolic reprogramming under hypothermia

We hypothesised that evolved cells would require an increase in metabolic resources to sustain their elevated volume, biomass content, proliferation rate, and mitochondrial capacity. This is supported by previous studies reporting the metabolic reprogramming of CHO cells

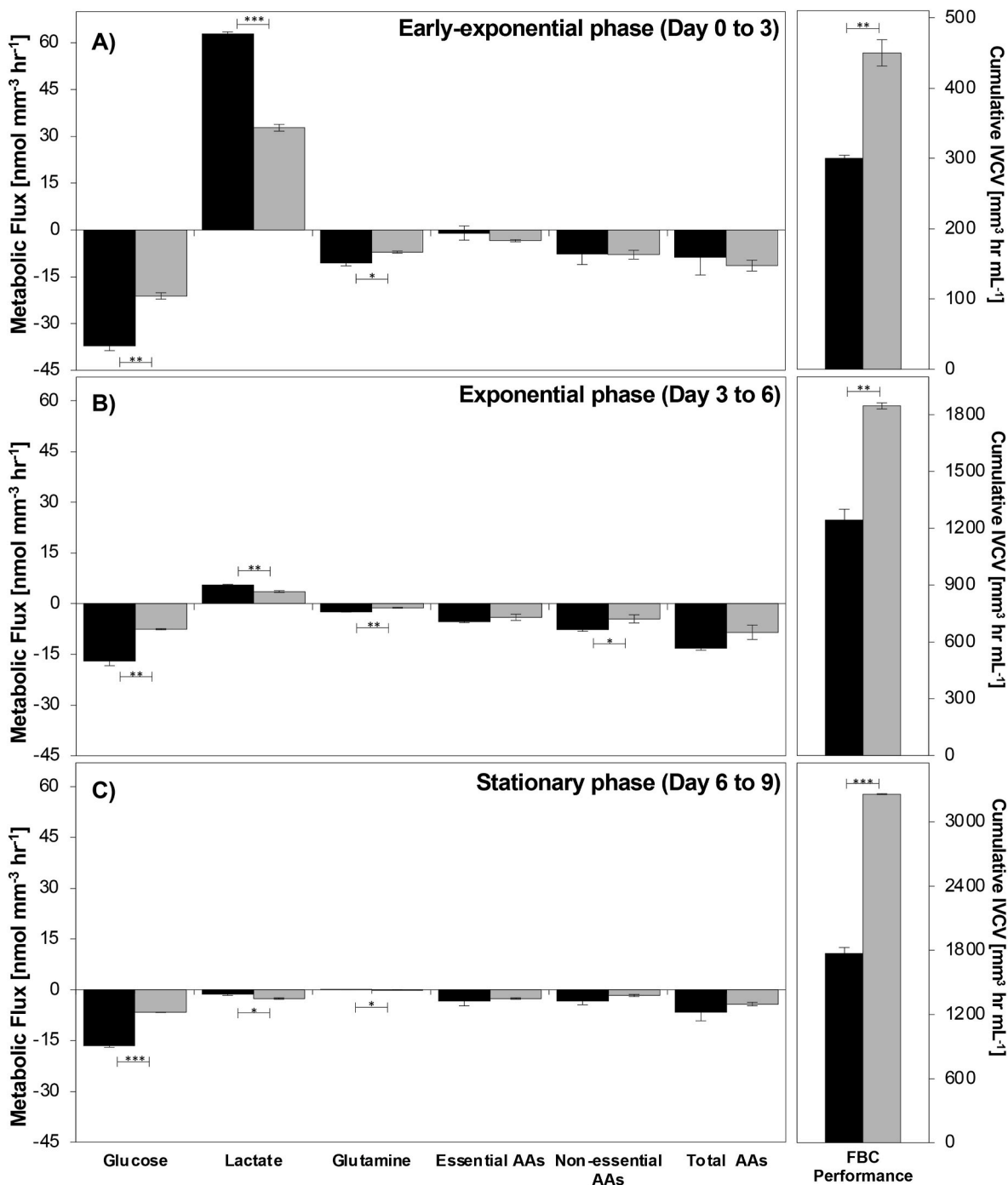


Fig. 4. Central carbon and amino acid metabolism of 37A and 32A cell populations. Cell supernatants were sampled at early exponential (A), exponential (B) and stationary (C) growth phases of FBC for the measurement of glucose, lactate, glutamine, and essential and non-essential amino acids. The cell-specific metabolic rates were calculated using the IVCV (displayed to the right of each plot) to exclude any cell volume effects. The black and grey bars represent the 37A and 32A cell populations, respectively. Statistical significance ($n = 3$) was calculated between 37A and 32A measurements of each metabolite at each culture phase sampling point by Student's *t*-test and is indicated as follows: * $P < 0.05$, ** $P < 0.01$, *** $P < 0.001$.

upon a shift to hypothermia (Wagstaff et al., 2013), particularly for the utilisation of major carbon and nitrogen sources, such as glucose, lactate and glutamine (Fogolin et al., 2004; Marchant et al., 2008). Therefore, we investigated the state of cellular metabolism within 37A and 32A cell populations at early-exponential (day 3 – Fig. 4A), exponential (day 6 – Fig. 4B) and stationary (day 9 – Fig. 4C) phases of FBC by measuring the cell-specific flux of major carbon sources (i.e., glucose and glutamine), by-products (lactate) and amino acids. To exclude cell volume effects, all measurements were corrected using the integral of viable cell volume (IVCV). Amino acids are displayed as either essential, non-essential or total.

During cell proliferation (Fig. 4A and B) 32A cells demonstrated reduced glucose uptake (2.2-fold) and lactate production (up to 1.9-fold) compared to 37A cells, revealing an altered carbon source utilisation and glycolytic activity. The uptake of glutamine, another critical CHO cell energy source, was also reduced (2-fold). Also, during cell proliferation, 32A cells exhibited a greater (1.3-fold) amino acid uptake than 37A cells during early-exponential phase (Fig. 4A), but a relatively reduced amino acid uptake (1.5-fold) during mid-exponential phase (Fig. 4B). During stationary phase (Fig. 4C) the overall metabolic flux was decreased for both 37A and 32A cells when compared to proliferative culture phases (Fig. 4A and B). When compared with 37A cells, 32A cells maintained their reduced glucose and amino acid uptake (2.5-fold and 1.9-fold, respectively). Net glutamine flux was near zero for both 37A and 32A cells, but the observation that 37A cells are producing glutamine and 32A cells are consuming glutamine is statistically significant ($p < 0.05$). Additionally, for both 37A and 32A cells, there was shift from net lactate production to net lactate consumption, a phenomenon that was more prominent in 32A cells (1.9-fold).

Taken together these analyses suggest that cell metabolism is significantly altered in response to hypothermic adaptation. Whilst these observations may demonstrate an optimisation of resource utilisation, the overall consumption of energy resources (i.e., glucose and glutamine) is decreased. Therefore, it is doubtful that these adaptations completely account for the increased biosynthetic and oxidative capacity of evolved cells. Consequently, we hypothesise that an alternative energy source in media such as fatty acids may provide additional resources for anabolism in cold-adapted cells, and that this would also be critical for the utilisation of adaptive non-shivering thermogenesis as a thermoregulatory mechanism (Klingenspor et al., 2008; El Bacha et al., 2010; Nicholls et al., 1986; Houten et al., 2016; Park et al., 2022).

3.5. Evolved cells exhibit superior biomanufacturing capabilities

To determine whether adaptation to 32 °C had impacted recombinant protein production we compared the transient and stable production of model IgG4 mAb and Fc-fusion proteins in both 37A and 32A cell populations.

Transient production of model IgG4 mAb and Fc-fusion proteins in 37A and 32A cells was assessed during a fed-batch process performed at both 37 °C and 32 °C (Fig. 5) after lipofectamine transfection. All transfections achieved consistent transfection efficiencies (50%–60%) and were not significantly different when comparing evolved and control cells (data not shown). Under their native temperatures (i.e., 37A cells at 37 °C and 32A cells at 32 °C) 32A cells outperformed 37A cells in terms of product titre (1.30- and 1.28-fold for IgG4 and Fc-fusion, respectively; Fig. 5A), however, IVCC performance was approximately similar (data not shown). At 32 °C, 32A cells outperformed 37A cells in terms of product titre (1.77- and 1.49- fold for IgG4 and Fc-fusion, respectively; Fig. 5A) and IVCC (2.56- and 2.60-fold for IgG4 and Fc-fusion, respectively; data not shown). Primarily, this appears to be due to the relatively poor ability of 37A cells to proliferate at 32 °C (Fig. 5C). At 37 °C 32A cells had relatively low product titres (0.37- and 0.36- fold for IgG4 and Fc-fusion, respectively; Fig. 5A) and IVCC (0.43- and 0.47-fold for IgG4 and Fc-fusion, respectively; data not shown) compared to 37A cells due to their shortened stationary phase and early decline in

VCC (Fig. 5B). 32A cells were able to achieve a biphasic culture profile across the fed-batch process at 32 °C (Fig. 5C), further demonstrating that evolved cells have similar proliferation characteristics to cells routinely cultured at 37 °C.

Triplicate stable cell pools producing IgG4 mAb and Fc-fusion protein were generated using both 37A and 32A cell populations, and their production under native temperatures was measured. Cells were transfected using electroporation. The average transfection efficiencies were ~95% and ~85% for 32A and 37A cells, respectively (data not shown), demonstrating an improvement in electroporation for evolved cells. 32A stable pools achieved larger product titres for both IgG4 mAb (1.14-fold; Fig. 6A) and Fc-fusion protein (1.72-fold; Fig. 6B) when compared to 37A pools. The volumetric titre difference between IgG4 mAb (272 mg L⁻¹) and Fc-fusion protein (202 mg L⁻¹) in 37A stable transfectant pools reflects the biosynthetic challenges imposed by these complex molecules, with the Fc-fusion protein being relatively more “difficult-to-express” (DTE). Notably, the 32A Fc-fusion stable pools outperformed the volumetric titre of both (37A and 32A) IgG4 stable pools (Fig. 6). This indicates that adaptation to 32 °C has a product-specific impact upon biomanufacturing performance and that the biosynthetic challenges related to the production of the model Fc-fusion protein production were more substantially alleviated by this adaptation in comparison to the model IgG4 protein.

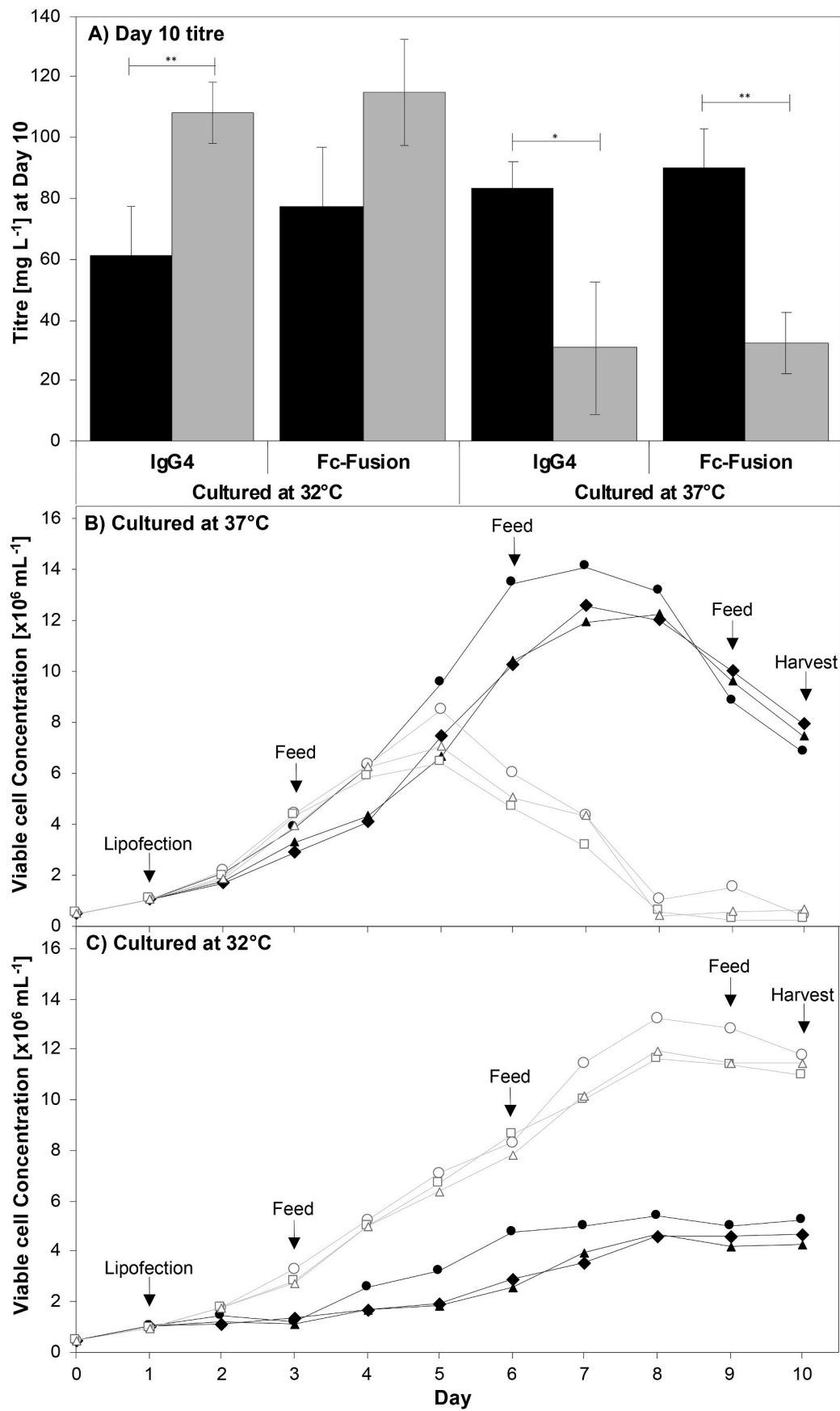
The profile of N-glycans is one of the main quality control attributes of mAbs and a key element during the selection of manufacturing host cell lines (O’Callaghan et al., 2015). N-glycan analyses by UPLC showed that there was no difference in N-glycan profiles between 37A and 32A pools producing IgG4 mAb or Fc-fusion proteins (Fig. 6A and B). These results indicate that the evolution process has not interfered with or adversely compromised N-glycan processing – a critical requirement when developing a new lead production cell line.

Taken together, these data ultimately show that the evolved cells are excellent host candidates for producing a large range of industrially relevant recombinant proteins.

3.6. Evolved cell functional adaptations correspond to gross changes in cellular mRNA abundance

We hypothesised that the multi-functional phenotypic divergence of evolved cells would be underpinned by large-scale changes in gene expression. Therefore, transcriptomic analysis of early-exponential (day 3) 32A and 37A cells was carried out via RNA-seq. A PCA plot of the RNA-seq data (Fig. 7A) shows that 37A and 32A cell populations have distinct gene expression profiles, with each population belonging to a distinct cluster. When comparing 37A and 32A populations almost half (993) of genes are significantly ($\text{Padj} < 0.05$) differentially expressed and 15% (1437) of these changes are ≥ 2 -fold ($\geq \log_2 +/ -1$; Fig. 7B). Differential expression was split evenly between upregulation and downregulation. Many of these substantial changes are related to critical cellular processes (Fig. 7C), including those that were found to be functionally different when comparing evolved and control cells, such as cell proliferation (cell cycle, apoptosis), DNA replication, biomass accumulation (translation, transcription, ribosome biogenesis, protein folding/assembly), mitochondrial activity (ETC, thermogenesis, redox control), cellular metabolism (fatty acids, lipids, amino acids), and recombinant protein production (translation, protein folding/assembly, protein transport).

Targeted analyses of pivotal genes that underpin cell cycle and energy metabolism (Fig. 8) elucidates the potential adaptive mechanisms that gave rise to the divergent functions of evolved cells during selection. Typically, the successful transition between cell cycle phases is driven by accumulation (through increased transcription) or degradation of various phase-specific cyclins: G1 phase – cyclin D, S phase and G1/S – cyclin E, G2 phase and G2/M – cyclin A, M phase – cyclins A and B (Cooper, 2000). 32A cells display significant changes in the expression of these cyclins and other critical checkpoint regulatory genes (Fig. 8A).



(caption on next page)

Fig. 5. Transient expression of IgG4 mAb and Fc-fusion protein in fed-batch culture. Plasmid DNA vectors encoding either recombinant IgG4 mAb or Fc-fusion protein were transfected into 37A and 32A cell populations in triplicate by lipofection. Transfected cells were assessed within a 10-day FBC at both 37 °C and 32 °C. **A)** Protein titres were measured at day 10 post-transfection. The black and grey bars represent the 37A and 32A populations, respectively. Statistical significance ($n = 3$) was calculated by Student's t-test and is indicated as follows: * $P < 0.05$, ** $P < 0.01$, *** $P < 0.001$. VCC measurements were taken daily for transfected populations grown at 37 °C **(B)** and 32 °C **(C)**. The black and grey lines represent each of the transfected 37A and 32A populations, respectively.

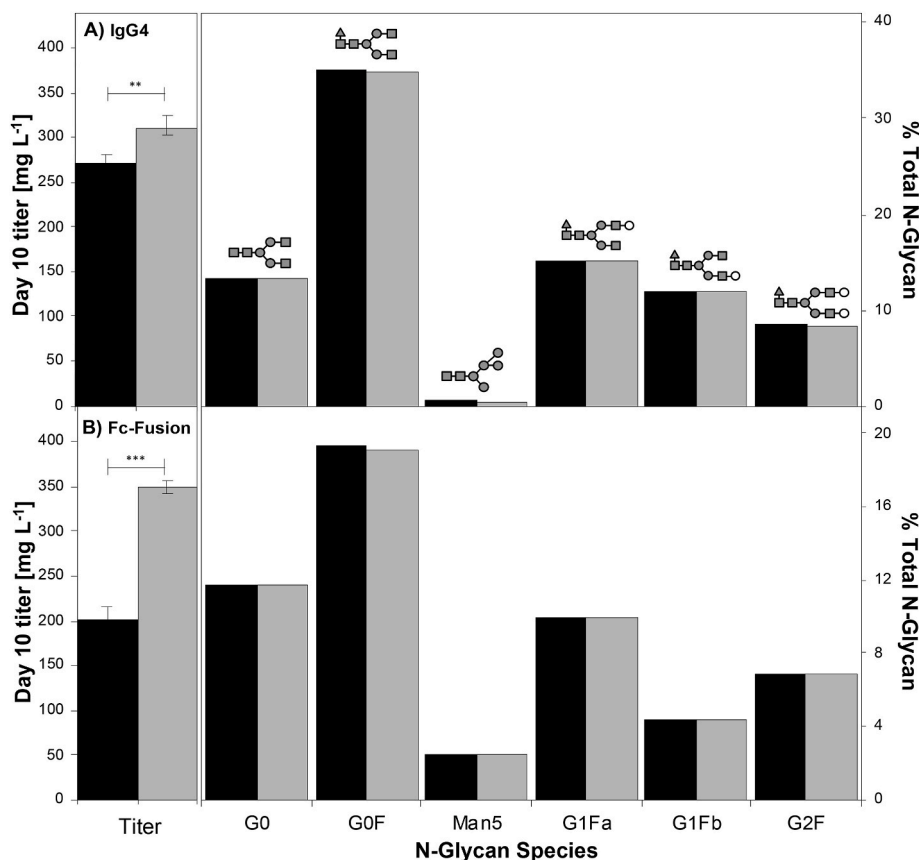


Fig. 6. Protein titres and N-glycan profiles from IgG4 mAb **(A)** and Fc-fusion protein **(B)** 37A and 32A stable transfectant pools under native culture temperatures (37A – 37 °C; 32A – 32 °C). Protein titres were measured at day 10 of FBC. The black and grey bars represent the 37A and 32A cell populations, respectively. Statistical significance ($n = 3$) between titre measurements was calculated by Student's t-test and is indicated as follows: * $P < 0.05$, ** $P < 0.01$, *** $P < 0.001$. The glycan schematics represent the N-glycan forms at day 10 of FBC ($n = 1$): G0, G0F, Man5, G1Fa, G1Fb or G2F (where the shapes represent the following: triangle: fucose, square: n-acetylglucosamine, clear circle: galactose, shaded circle: mannose). The black and grey bars represent the 37A and 32A populations, respectively.

Specifically, the slow G1 phase displayed by 32A cells is in line with the decreased expression of cyclin D, cyclin E and Rb, as well as increased expression of E2f1, E2f2 and HDAC, which together are associated with a delayed commitment to G1/S transition (van den Heuvel and Dyson, 2008; Bertoli et al., 2013; Hai et al., 2021). Also, increased expression of Cyclin A, Cyclin B, CDKs and other key regulators (e.g., Cdc20, Cdc25, 14-3-3) correspond to the relatively quicker evolved cell progression through S, G2 and M phases (Hochegger et al., 2008). In addition, differential expression of genes related to DNA replication, microtubule organisation, and spindle formation could explain the increased levels of chromosomal instability and aneuploidy found in evolved cells (Zimmet and Ravid, 2000; Jahn et al., 2013; Wang et al., 2020).

Differential gene expression within relevant functional modules (amino acid metabolism, glucose/glutamine metabolism; Fig. 7C) support our findings (Fig. 4) that metabolism of major energy sources (i.e., glucose and glutamine), by-products (lactate) and amino acids is altered. As previously mentioned, we hypothesise that these alterations are not sufficient to support the increased capacity of evolved cells. Fig. 7C also shows substantial differential gene expression in lipid and fatty acid metabolism in 32A cells and so we carried out a targeted analysis to establish whether these processes could be meeting the elevated demands of the evolved cell phenotype. Indeed, there is substantial

differential gene expression in 32A cells (Fig. 8B) that suggests elevated lipid-based energy metabolism through increased fatty acid uptake, β -oxidation, and entry into the TCA cycle. It also suggests that *de novo* fatty acid and lipid synthesis are increased, alongside increased lipolysis (breakdown of lipids into fatty acids), which would provide further resource for these processes. Together, these elevated processes would facilitate higher levels of respiration and oxidative phosphorylation in the mitochondria, which also display large differences in gene expression. Also, in line with our experimental data, there is a decrease in expression of genes related to mitochondrial ROS production alongside an increase in expression of genes related to the mitochondrial antioxidant response and mild ROS maintenance (Fig. 8B).

4. Discussion

After prolonged (over 150 generations) exposure to 32 °C in shake-flasks, CHO cells displayed extensive functional adaptations to enable proliferation in hypothermic conditions, and this adaptation was associated with genome-scale changes in cellular mRNA abundance and karyotype. As a result, the evolved cell functional landscape was markedly different to that of the parental host, ultimately giving rise to superior biomanufacturing performance characteristics.

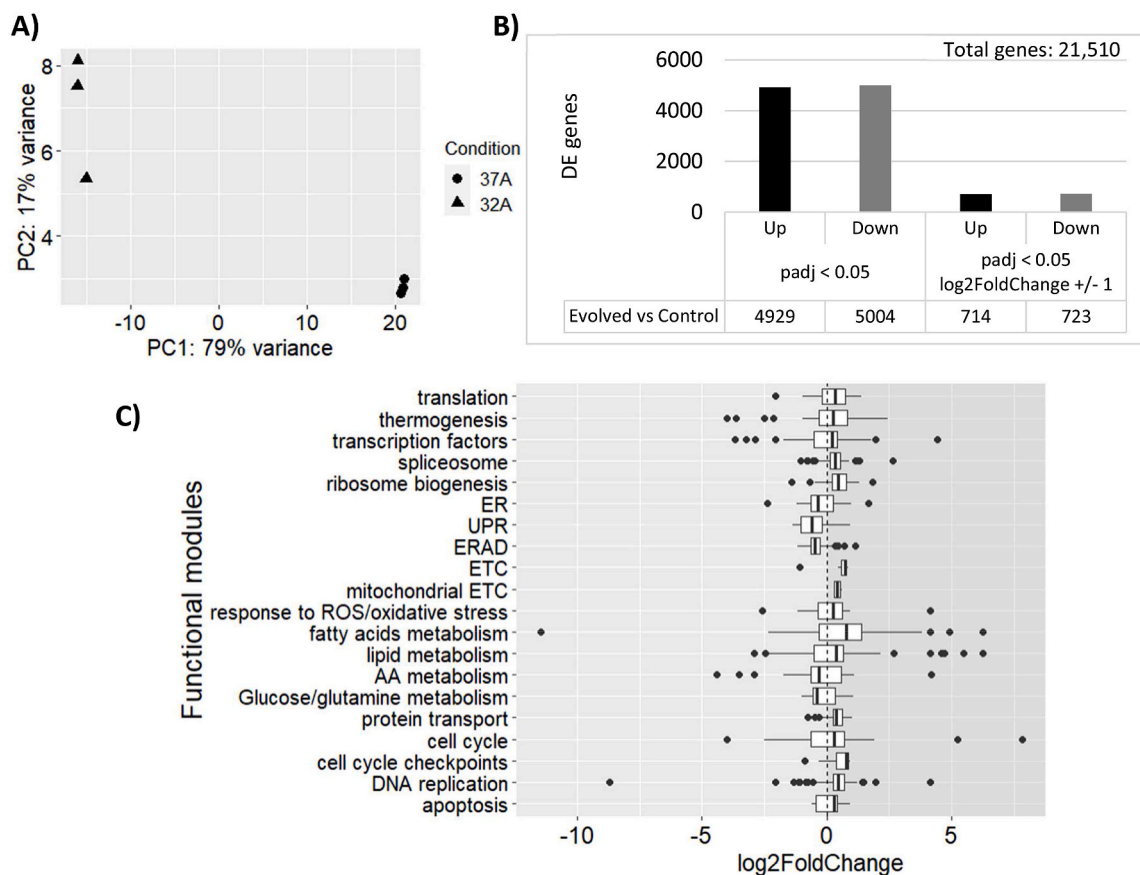


Fig. 7. Differential gene expression between 37A and 32A cell populations. Triplicate samples were taken from mid-exponential phase 37A and 32A cell populations for RNAseq analysis. **A)** PCA plot showing the clustering of 37A and 32A cells relative to their differing gene expression profiles. **B)** The number of significantly differentially expressed genes (Padj < 0.05) in 37A and 32A cell populations, with and without a log2FC cut-off of +/-1. The total number of CHO genes is shown for context. **C)** Functional module (based on GO terms and KEGG pathways) gene expression differences (log2 fold change) in 32A cells compared to 37A cells.

The increase in proliferation rate and cell volume in evolved cells suggests that alterations to control of cell cycling were a critical factor for hypothermic adaptation. To enable proliferation at the same rate as cells routinely cultured at 37 °C, evolved cells needed to overcome 32°C-induced cell cycle arrest in G1 (Fogolin et al., 2004; Hendrick et al., 2001; Kaufmann et al., 1999; Marchant et al., 2008; Moore et al., 1997; Rieder and Cole, 2002). Cells arrested in G1 phase are generally more metabolically active, accumulate more biomass, are significantly larger, and are more productive (Bi et al., 2004; Carvalhal et al., 2003; Ginzberg et al., 2015; Son et al., 2012). In evolved cells the rate of G1 transition did recover but was still slower than that of cells cultured at 37 °C. However, a slow G1 was compensated by a rapid rate of transition from S to M phase, resulting in an overall recovery in proliferation rate. These changes in cell cycle progression resulted in biosynthetically enhanced cells that maintained the cellular phenotypes inherent within G1 arrest without compromising doubling time. The increase in RNA and protein content supports previous findings that global transcriptional and translational rates scale with cell volume (Dungrawala et al., 2010; Marguerat and Baehler, 2012; Padovan-Merhar et al., 2015; Zhurinsky et al., 2010), although a slower rate of biomass turnover at sub-physiological temperatures might also explain the accumulation of cellular biomass content. Increased cell volume could also be interpreted as a thermodynamic stress response intended to reduce heat loss by a reduction in surface area to volume ratio (Meiri and Dayan, 2003; Sand et al., 1995).

The comprehensive changes in cell cycle progression coincided with a dysregulation of the requisite checkpoints that govern cell division fidelity, such as those controlling the proper replication and division of genetic material. Indeed, a rapid transition from S phase to mitosis has

previously been shown to increase errors in genomic repair and chromosome segregation (Hartwell and Kastan, 1994; Lobrich and Jeggo, 2007; Knauf et al., 2006) and the increased levels of chromosomal instability (CIN) in evolved cells represents a loss of fidelity in these processes (Thompson et al., 2010). Chromosome segregation is a precise, highly coordinated, and multigenic process which can be severely impacted by changes in expression of its regulatory genes (Hochegger et al., 2008; Malumbres and Barbacid, 2009; Jahn et al., 2013). Various instances of differential gene expression in evolved cells (Fig. 8A) point towards increased chromosomal instability, such as increased expression of Cyclin A (Tane and Chibazakura, 2009), dysregulation of mini-chromosome maintenance (MCM) proteins (Bailis and Forsburg, 2004), and decreased *Map9* gene expression (Wang et al., 2020). Interestingly, larger cells are prone to spindle positioning defects, resulting in chromosome mis-segregation and aneuploidy (Cadart et al., 2014). Aneuploidy led to increased genetic variation within the evolved cell population, associated with cellular adaptation to hypothermia. Therefore, genomic variability and plasticity, through mechanisms such as high CIN, could be adaptive prerequisites to accelerate and promote cellular adaptation via directed evolution approaches, permitting creation of more robust mammalian phenotypes for industrial applications. In accordance with this, it has been shown that aneuploidy in mammalian cells can function as a mechanism to adapt to stressful environments and gain a proliferative advantage (Duncan et al., 2012). This is supported by evolutionary studies in cancer cells that have shown that CIN and aneuploidy can facilitate adaptation to detrimental environments and cause drug resistance (Sansregret and Swanton, 2017).

The elevated biosynthetic capabilities of evolved cells are supported by an increased mitochondrial oxidative capacity (Fig. 3). Recent CHO

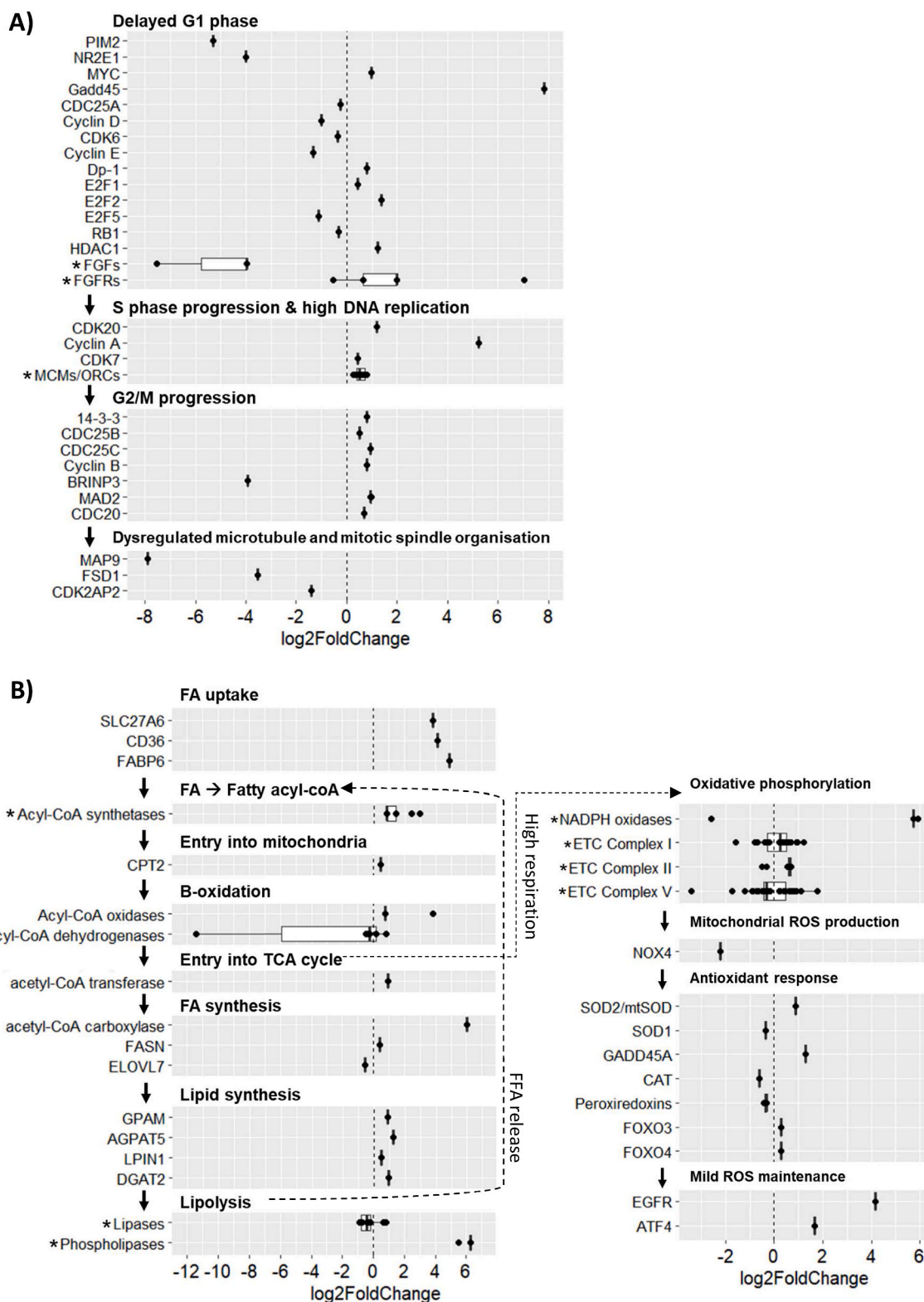


Fig. 8. Differential gene expression analysis of cell cycle and energy metabolism between 37A and 32A cell populations. Differential expression of genes in 32A cells is displayed in terms of their log₂ fold change in expression in comparison with 37A cells. **(A)** Changes in the expression of genes specifically involved in cell cycle-related processes: delayed G1 phase; S phase progression & high DNA replication; G2/M progression; and dysregulated microtubule and mitotic spindle organisation. **(B)** Changes in the expression of genes specifically involved in lipid, fatty acid, and mitochondrial processes: fatty acid uptake; fatty acid conversion to fatty acyl-coA; entry of fatty acyl-coA into the mitochondria; β-oxidation of fatty acids; entry of acetyl-coA into the TCA cycle; fatty acid synthesis; lipid synthesis; lipolysis; oxidative phosphorylation; mitochondrial ROS production, antioxidant response; and mild ROS maintenance. For instances where more than one gene has been included within a single boxplot the name within the axis label represents a group of genes and is preceded by *.

cell studies have demonstrated that early activation of mitochondrial metabolism and a healthy oxidative mitochondrial capacity are necessary to sustain an intensive biosynthetic capacity (Fernandez-Martell et al., 2018) and to increase recombinant protein production (Templeton et al., 2013), which is indicative of the substantial energy requirement of recombinant protein synthesis. Furthermore, energy limitation has been shown to be a bottleneck for recombinant protein production, particularly for DTE proteins (Martinez et al., 2016; Gutierrez et al., 2020; Park et al., 2022). Production of ROS has been shown to scale with mitochondrial activity (Doherty and Cleveland, 2013), but here we show that evolved cells have mitigated this toxic by-product of increased biosynthetic capacity with an increase in antioxidant capacity (Fig. 3B). ROS mitigation is a desirable trait for a biomanufacturing cell line and a recent study showed that CHO cells evolved to have an increased antioxidant capacity displayed increased growth, viability, and bispecific antibody production in FBC (Mistry et al., 2021).

Differential utilisation of carbon and nitrogen sources in evolved cells (Fig. 4) likely contributed to their enhanced biomanufacturing capabilities by sustaining their increased capacity for proliferation, biomass accumulation and energy metabolism (Ghorbaniaghdam et al., 2014; Lukey et al., 2017; Geoghegan et al., 2018; Park et al., 2022). For example, evolved cells display a more pronounced shift towards net lactate consumption in stationary phase when compared to cells maintained at 37 °C, which has been associated with enhanced culture performance (Dorai et al., 2009) and increased productivity (Le et al., 2012; Templeton et al., 2013; Park et al., 2022). Moreover, the mitigation of lactate as a toxic by-product, by the rewiring of lactate resorption during stationary phase and a reduced reliance upon glucose (allowing a lower production of lactate) throughout FBC, is an example of system detoxification. However, we suggest that the change in carbon and nitrogen source utilisation would not be sufficient to solely sustain this evolved enhanced biosynthetic capacity. Based upon our transcriptomic analysis (Fig. 8B) we speculate that lipid and fatty acid metabolism was completely rewired to become a critical resource for evolved cells. Specifically, it indicates that evolved cells have increased levels of free fatty acids via increased fatty acid uptake, fatty acid and lipid *de novo* synthesis, and lipid lipolysis. The conversion of fatty acids to fatty acyl-CoA, entry of fatty acyl-CoA into the mitochondria, β -oxidation of fatty acyl-CoA, and entry of the resulting acetyl-CoA into the TCA cycle all also appear to be elevated according to the transcriptomic data. The resulting increased levels of NADH and FADH₂ from both the β -oxidation and the TCA cycle would be a substantial contributor to the elevated activity of the mitochondrial electron transport chain (Toleikis et al., 2020). In line with these findings previous studies that have shown that fatty acid metabolism is elevated during stressful conditions such as cold exposure and starvation (i.e., low carbon source utilisation), providing a critical source of energy and overall anabolic biomass accumulation (Nicholls et al., 1986; Houten et al., 2016; Park et al., 2022). Furthermore, under Warburg states, proliferating cells have been shown to scavenge free fatty acids from surrounding media to maintain a constant supply of biomass precursors (Kamphorst et al., 2013), cofactors (Keibler et al., 2016), and anaplerotic intermediates (Liu, 2006). Therefore, our study highlights that the positive regulation of mitochondrial oxidative capacity in evolved cells is likely to be closely associated with increased mitochondrial biogenesis and fatty acid catabolism. This is supported by numerous studies that have sought to engineer mitochondrial metabolism with key regulators such as PGC-1 α , which improved metabolic fitness during stress conditions (Canto and Auwerx, 2009), and increased mitochondrial oxidative capacity and fatty acid β -oxidation (St-Pierre et al., 2006; Xu et al., 2016). Although we did not measure free fatty acids or acetyl-CoA concentrations, these observations indicate that evolved cells utilised alternative readily available medium components other than glucose and amino acids (e.g., free fatty acids) as nutrient sources for oxidative metabolism and as building blocks for rapid synthesis and maintenance of cellular biomass.

Corresponding changes in energy metabolism, ROS mitigation and

fatty acid metabolism also indicate another form of thermoregulation in evolved cells - non-shivering thermogenesis (Rial and Zardoya, 2009; Stier et al., 2014; Zhang et al., 2021), whereby free fatty acids stimulate mitochondrial uncoupling proteins (UCPs) to increase proton motive force allowing cells to dissipate energy as heat (Klingenspor et al., 2008). In line with the increased volume of evolved cells, it has been shown that stress-related cell size increases can trigger UCP activation via the release of long-chain fatty acids from the mitochondrial membrane by phospholipase A2 (Kiehl et al., 2011; Klingenspor et al., 2008; Lambert et al., 2006; Rial and Zardoya, 2009). As well as increasing metabolic fitness and oxidative metabolism, the engineering of mitochondrial metabolism with the PGC-1 α regulator also facilitated non-shivering thermogenesis (Puigserver et al., 1998). Therefore, the necessity to generate heat could have been a key evolutionary driver stimulate the drastic metabolic changes observed in evolved cells.

Here we have shown that hypothermic adaptation is potentially an effective methodology to propel CHO cells towards an inherently more effective biomanufacturing phenotype. Directed evolution, or adaptive selection, is advantageous because it yields new cell populations with numerous coordinated alterations across many cellular functional modules (Sinacore et al., 2000; Prentice et al., 2007; Sunley et al., 2008; Bort et al., 2010; Costa et al., 2011; Fernandez-Martell et al., 2018; Chandrawanshi et al., 2020; Weinguny et al., 2020; Mistry et al., 2021; Chakrabarti et al., 2022). The extent of change can be clearly seen by the scale of karyotypic and transcriptomic changes that underpin the functional transformation of evolved cells. The extent and breadth of functional changes in evolved cells is vast, all of which have previously been associated with improvements in biomanufacturing performance: increased cell size (Bi et al., 2004; Carvalho et al., 2003; Dreesen and Fussenegger, 2011; Kiehl et al., 2011); increased biomass content (Edros et al., 2013; Khoo and Al-Rubeai, 2009); changes in cell cycle regulation (Dutton et al., 2006; Park et al., 2016); increased mitochondrial energy metabolism (Fernandez-Martell et al., 2018; Templeton et al., 2013; Chakrabarti et al., 2022); increased antioxidant capacity and decreased ROS (Mistry et al., 2021); altered carbon metabolism (Toussaint et al., 2016); altered amino acid metabolism (Xing et al., 2011; Fan et al., 2015); and increased lipid and fatty acid metabolism (Budge et al., 2020; Coronel et al., 2016). Of course, these findings provide additional evidence that these cellular functions could be targeted for enhancement via focussed engineering approaches (e.g., genetic, process, or media engineering). However, the salient conclusions here are that CHO cell plasticity and heterogeneity is perhaps the most beneficial resource to be harnessed for the creation of generically efficacious cell factories and that directed evolution or selection-based methods can be easily employed to utilise it. Of course, to take any adapted cell population forward as a production host it would need to possess the necessary qualities for commercial manufacture, such as bioreactor compatibility and stability. In particular, the latter may come under scrutiny given the extent of genetic changes that are apparently required for adaptation.

In applying this strategy to generally improve CHO cell performance, our data should be interpreted with a final note of caution. Whilst our data do clearly illustrate that directed selective pressures can promote progressive outgrowth of functionally different cell phenotypes, there may be a requirement for permissive genetic variants to exist (even at very low frequency) within a genetically heterogeneous founder population, such as Lonza CHOK1SV® (Fan et al., 2013). Correspondingly, we have previously shown that this heterogeneity can be exploited to generate superior clonal derivatives for biomanufacturing (Davies et al., 2013). Transformed cell types such as CHO will accumulate genetic variation, but clonally derived cultures lacking extensive genetic heterogeneity may lack the requisite variant permissive founder cells for this approach to be successful. Therefore, the rate of adaptation to a selective pressure and the evolutionary outcome may vary by population and so different populations might require divergent adaptive strategies. In this respect, the use of directed evolution/adaptation as an approach to engineering cell performance differs from targeted genetic

engineering. However, even with respect to the latter, the efficacy of specific genetic changes will likely be entirely dependent on cellular genetic context.

Declarations of interest

The authors declare no competing interests.

Funding

BBSRC studentship and sponsorship by Lonza Biologics.

Author statement

Katie L. Syddall: Conceptualisation, Data curation, Formal analysis, Investigation, Methodology, Validation, Visualization, Writing - original draft, Writing - review & editing. **Alejandro Fernandez-Martell:** Conceptualisation, Data curation, Formal analysis, Investigation, Methodology, Validation, Visualization, Writing - original draft, Writing - review & editing. **Joseph F. Cartwright:** Conceptualisation, Visualization, Writing - original draft, Writing - review & editing. **Cristina N. Alexandru-Crivac:** Data curation, Formal analysis, Investigation, Methodology, Visualization, Writing - review & editing. **Adam Hodgson:** **Andrew J. Racher:** Conceptualisation, Writing - review & editing, Supervision, Project administration, Funding acquisition, Resources. **Robert J. Young:** Conceptualisation, Writing - review & editing, Supervision, Project administration, Funding acquisition, Resources. **David C. James:** Conceptualisation, Methodology, Writing - review & editing, Supervision, Project administration, Funding acquisition.

Data availability

The authors do not have permission to share data.

Acknowledgements

We would like to acknowledge Dr. Mark Dunning from Sheffield Bioinformatics Core for advice and support with pre-processing of RNA-seq data.

References

- Ahn, W.S., Jeon, J.-J., Jeong, Y.-R., Lee, S.J., Yoon, S.K., 2008. Effect of culture temperature on erythropoietin production and glycosylation in a perfusion culture of recombinant CHO cells. *Biotechnol. Bioeng.* 101, 1234–1244.
- Al-Fageeh, M.B., Marchant, R.J., Carden, M.J., Smales, C.M., 2006. The cold-shock response in cultured mammalian cells: harnessing the response for the improvement of recombinant protein production. *Biotechnol. Bioeng.* 93, 829–835.
- Ashburner, M., Ball, C.A., Blake, J.A., Botstein, D., Butler, H., Cherry, J.M., Davis, A.P., Dolinski, K., Dwight, S.S., Eppig, J.T., Harris, M.A., Hill, D.P., Issel-Tarver, L., Kasarskis, A., Lewis, S., Matese, J.C., Richardson, J.E., Ringwald, M., Rubin, G.M., Sherlock, G., Consortium, G.O., 2000. Gene Ontology: tool for the unification of biology. *Nat. Genet.* 25, 25–29.
- Bailis, J.M., Forsburg, S.L., 2004. MCM proteins: DNA damage, mutagenesis and repair. *Curr. Opin. Genet. Dev.* 14, 17–21.
- Balaban, R.S., Nemoto, S., Finkel, T., 2005. Mitochondria, oxidants, and aging. *Cell* 120, 483–495.
- Bertoli, C., Skotheim, J.M., De Bruin, R.A.M., 2013. Control of cell cycle transcription during G1 and S phases. *Nat. Rev. Mol. Cell Biol.* 14, 518–528.
- Bi, J.X., Shuttleworth, J., Ai-Rubeai, M., 2004. Uncoupling of cell growth and proliferation results in enhancement of productivity in p21(C1P1)-arrested CHO cells. *Biotechnol. Bioeng.* 85, 741–749.
- Bort, J.a.H., Stern, B., Borth, N., 2010. CHO-K1 host cells adapted to growth in glutamine-free medium by FACS-assisted evolution. *Biotechnol. J.* 5, 1090–1097.
- Brand, M.D., Nicholls, D.G., 2011. Assessing mitochondrial dysfunction in cells (vol 435, pg 297, 2011). *Biochem. J.* 437, 575–575.
- Budge, J.D., Knight, T.J., Povey, J., Roobol, J., Brown, I.R., Singh, G., Dean, A., Turner, S., Jaques, C.M., Young, R.J., Racher, A.J., Smales, C.M., 2020. Engineering of Chinese hamster ovary cell lipid metabolism results in an expanded ER and enhanced recombinant biotherapeutic protein production. *Metab. Eng.* 57, 203–216.
- Cadart, C., Zlotek-Zlotkiewicz, E., Le Berre, M., Piel, M., Matthews, H.K., 2014. Exploring the function of cell shape and size during mitosis. *Dev. Cell* 29, 159–169.
- Canto, C., Auwerx, J., 2009. PGC-1 alpha, SIRT1 and AMPK, an energy sensing network that controls energy expenditure. *Curr. Opin. Lipidol.* 20, 98–105.
- Carbon, S., Douglass, E., Good, B.M., Unni, D.R., Harris, N.L., Mungall, C.J., Basu, S., Chisholm, R.L., Dodson, R.J., Hartline, E., Fey, P., Thomas, P.D., Albou, L.P., Ebert, D., Kesling, M.J., Mi, H.Y., Muruganujan, A., Huang, X.S., Mushayahama, T., Labonte, S.A., Siegele, D.A., Antonazzo, G., Attrill, H., Brown, N.H., Garapati, P., Marygold, S.J., Trovisco, V., Dos Santos, G., Falls, K., Tabone, C., Zhou, P.L., Goodman, J.L., Strelets, V.B., Thurmond, J., Garmiri, P., Ishtiaq, R., Rodriguez-Lopez, M., Acencio, M.L., Kuiper, M., Laegreid, A., Logie, C., Lovering, R.C., Kramarz, B., Saverimuttu, S.C.C., Pinheiro, S.M., Gunn, H., Su, R.Z., Thurlow, K.E., Chibucos, M., Giglio, M., Nadendla, S., Munro, J., Jackson, R., Duesbury, M.J., Del-Toro, N., Meldal, B.H.M., Paneerselvam, K., Perfetto, L., Porras, P., Orchard, S., Shrivastava, A., Chang, H.Y., Finn, R.D., Mitchell, A.L., Rawlings, N.D., Richardson, L., Sangrador-Vegas, A., Blake, J.A., Christie, K.R., Dolan, M.E., Drabkin, H.J., Hill, D.P., Ni, L., Sitnikov, D.M., Harris, M.A., Oliver, S.G., Rutherford, K., Wood, V., Hayles, J., Bahler, J., Bolton, E.R., De Pons, J.L., Dwinell, M.R., Hayman, G.T., Kaldunski, M.L., Kwitek, A.E., Laulederkind, S.J.F., Plasterer, C., Tutaj, M.A., Vedi, M., Wang, S.J., D'eustachio, P., Matthews, L., Balhoff, J.P., Aleksander, S.A., Alexander, M.J., Cherry, J.M., Engel, S.R., Gondwe, F., Karra, K., et al., 2021. The Gene Ontology resource: enriching a GOLD mine. *Nucleic Acids Res.* 49, D325–D334.
- Carvalho, A.V., Marcelino, L., Carrondo, M.J.T., 2003. Metabolic changes during cell growth inhibition by p27 overexpression. *Appl. Microbiol. Biotechnol.* 63, 164–173.
- Chakrabarti, L., Chaerkady, R., Wang, J., Weng, S.H.S., Wang, C., Qian, C., Cazares, L., Hess, S., Amaya, P., Zhu, J., Hatton, D., 2022. Mitochondrial membrane potential-enriched CHO host: a novel and powerful tool for improving biomanufacturing capability. *mAbs* 14.
- Chandrawanshi, V., Kulkarni, R., Prabhu, A., Mehra, S., 2020. Enhancing titers and productivity of rCHO clones with a combination of an optimized fed-batch process and ER-stress adaptation. *J. Biotechnol.* 311, 49–58.
- Cooper, G.M., 2000. *The Cell: a Molecular Approach*. Sinauer Associates, Sunderland, MA.
- Coronel, J., Klausung, S., Heinrich, C., Noll, T., Figueredo-Cardero, A., Castilho, L.R., 2016. Valeric acid supplementation combined to mild hypothermia increases productivity in CHO cell cultivations. *Biochem. Eng. J.* 114, 104–112.
- Costa, A.R., Rodrigues, M.E., Henriques, M., Oliveira, R., Azeredo, J., 2011. Strategies for adaptation of mAb-producing CHO cells to serum-free medium. *BMC Proc.* 5 (Suppl. 8), P112–P112.
- Dahodwala, H., Lee, K.H., 2019. The fickle CHO: a review of the causes, implications, and potential alleviation of the CHO cell line instability problem. *Curr. Opin. Biotechnol.* 60, 128–137.
- Das Neves, R.P., Jones, N.S., Andreu, L., Gupta, R., Enver, T., Iborra, F.J., 2010. Connecting variability in global transcription rate to mitochondrial variability. *PLoS Biol.* 8.
- Davies, S.L., Lovelady, C.S., Grainger, R.K., Racher, A.J., Young, R.J., James, D.C., 2013. Functional heterogeneity and heritability in CHO cell populations. *Biotechnol. Bioeng.* 110, 260–274.
- Desler, C., Hansen, T.L., Frederiksen, J.B., Marcker, M.L., Singh, K.K., Juel Rasmussen, L., 2012. Is there a link between mitochondrial reserve respiratory capacity and aging? *Journal of aging research* 2012, 192503–192503.
- Dobin, A., Davis, C.A., Schlesinger, F., Drenkow, J., Zaleski, C., Jha, S., Batut, P., Chaisson, M., Gingeras, T.R., 2013. STAR: ultrafast universal RNA-seq aligner. *Bioinformatics* 29, 15–21.
- Doherty, J.R., Cleveland, J.L., 2013. Targeting lactate metabolism for cancer therapeutics. *J. Clin. Invest.* 123, 3685–3692.
- Dorai, H., Kyung, Y.S., Ellis, D., Kinney, C., Lin, C.B., Jan, D., Moore, G., Betenbaugh, M. J., 2009. Expression of anti-apoptosis genes alters lactate metabolism of Chinese hamster ovary cells in culture. *Biotechnol. Bioeng.* 103, 592–608.
- Dreesen, I.a.J., Fussenegger, M., 2011. Ectopic expression of human mTOR increases viability, robustness, cell size, proliferation, and antibody production of Chinese hamster ovary cells. *Biotechnol. Bioeng.* 108, 853–866.
- Duncan, A.W., Newell, A.E.H., Bi, W., Finegold, M.J., Olson, S.B., Beaudet, A.L., Grompe, M., 2012. Aneuploidy as a mechanism for stress-induced liver adaptation. *J. Clin. Invest.* 122, 3307–3315.
- Dungrawala, H., Manukyan, A., Schneider, B.L., 2010. Gene regulation: global transcription rates scale with size. *Curr. Biol.* 20, R979–R981.
- Dutton, R.L., Scharer, J., Moo-Young, M., 2006. Cell cycle phase dependent productivity of a recombinant Chinese hamster ovary cell line. *Cytotechnology* 52, 55–69.
- Edros, R.Z., McDonnell, S., Al-Rubeai, M., 2013. Using molecular markers to characterize productivity in Chinese hamster ovary cell lines. *PLoS One* 8.
- El Bacha, T., Luz, M.R.M.P., Da Poian, A., 2010. Dynamic adaptation of nutrient utilization in humans. *Nature Education* 3.
- Fan, L., Frye, C.C., Racher, A.J., 2013. The use of glutamine synthetase as a selection marker: recent advances in Chinese hamster ovary cell line generation processes. *Pharmaceutical Bioprocessing* 1, 487–502.
- Fan, Y., Del Val, I.J., Muller, C., Sen, J.W., Rasmussen, S.K., Kontoravdi, C., Weiguny, D., Andersen, M.R., 2015. Amino acid and glucose metabolism in fed-batch CHO cell culture affects antibody production and glycosylation. *Biotechnol. Bioeng.* 112, 521–535.
- Fedorenko, A., Lishko, P.V., Kirichok, Y., 2012. Mechanism of fatty-acid-dependent UCP1 uncoupling in Brown fat mitochondria. *Cell* 151, 400–413.
- Fernandez-Martell, A., Johari, Y.B., James, D.C., 2018. Metabolic phenotyping of CHO cells varying in cellular biomass accumulation and maintenance during fed-batch culture. *Biotechnol. Bioeng.* 115, 645–660.

- Fogolin, M.B., Wagner, R., Etcheverrigaray, M., Kratje, R., 2004. Impact of temperature reduction and expression of yeast pyruvate carboxylase on hGM-CSF-producing CHO cells. *J. Biotechnol.* 109, 179–191.
- Fox, S.R., Patel, U.A., Yap, M.G.S., Wang, D.I.C., 2004. Maximizing interferon-gamma production by Chinese hamster ovary cells through temperature shift optimization: experimental and modeling. *Biotechnol. Bioeng.* 85, 177–184.
- Geoghegan, D., Arnall, C., Hatton, D., Noble-Longster, J., Sellick, C., Senussi, T., James, D.C., 2018. Control of amino acid transport into Chinese hamster ovary cells. *Biotechnol. Bioeng.* 115, 2908–2929.
- Ghorbaniaghdam, A., Henry, O., Jolicoeur, M., 2014. An in-silico study of the regulation of CHO cells glycolysis. *J. Theor. Biol.* 357, 112–122.
- Gillooly, J.F., Hein, A., Damiani, R., 2015. Nuclear DNA content varies with cell size across human cell types. *Cold Spring Harbor Perspect. Biol.* 7.
- Ginzberg, M.B., Kafri, R., Kirschner, M., 2015. On being the right (cell) size. *Science* 348.
- Gomes, J.M., Hiller, G.W., 2018. Use of Low Temperature And/or Low pH in Cell Culture. US Patent. US9988662B2.
- Greene, D., Richardson, S., Turro, E., 2017. ontologyX: a suite of R packages for working with ontological data. *Bioinformatics* 33, 1104–1106.
- Gutierrez, J.M., Feizi, A., Li, S.Z., Kallehauge, T.B., Hefzi, H., Grav, L.M., Ley, D., Hizal, D.B., Betenbaugh, M.J., Voldborg, B., Kildegaard, H.F., Lee, G.M., Palsson, B. O., Nielsen, J., Lewis, N.E., 2020. Genome-scale reconstructions of the mammalian secretory pathway predict metabolic costs and limitations of protein secretion. *Nat. Commun.* 11.
- Hai, R.H., He, L.E., Shu, G., Yin, G., 2021. Characterization of histone deacetylase mechanisms in cancer development. *Front. Oncol.* 11.
- Handlogten, M.W., Lee-O'Brien, A., Roy, G., Levitskaya, S.V., Venkat, R., Singh, S., Ahuja, S., 2018. Intracellular response to process optimization and impact on productivity and product aggregates for a high-titer CHO cell process. *Biotechnol. Bioeng.* 115, 126–138.
- Hartwell, L.H., Kastan, M.B., 1994. CELL-CYCLE control and cancer. *Science* 266, 1821–1828.
- Hendrick, V., Winnepenninckx, P., Abdelkafi, C., Vandeputte, O., Cherlet, M., Marique, T., Renemann, G., Loa, A., Kretzmer, G., Werenne, J., 2001. Increased productivity of recombinant tissular plasminogen activator (t-PA) by butyrate and shift of temperature: a cell cycle phases analysis. *Cytotechnology* 36, 71–83.
- Hochegger, H., Takeda, S., Hunt, T., 2008. Cyclin-dependent kinases and cell-cycle transitions: does one fit all? *Nat. Rev. Mol. Cell Biol.* 9, 910–926.
- Houten, S.M., Violante, S., Ventura, F.V., Wanders, R.J., 2016. The biochemistry and physiology of mitochondrial fatty acid β -oxidation and its genetic disorders. *Annu. Rev. Physiol.* 78, 23–44.
- Jahn, S.C., Corsino, P.E., Davis, B.J., Law, M.E., Norgaard, P., Law, B.K., 2013. Constitutive Cdk2 activity promotes aneuploidy while altering the spindle assembly and tetraploidy checkpoints. *J. Cell Sci.* 126, 1207–1217.
- Kamphorst, J.J., Cross, J.R., Fan, J., De Stanchina, E., Mathew, R., White, E.P., Thompson, C.B., Rabinowitz, J.D., 2013. Hypoxic and Ras-transformed cells support growth by scavenging unsaturated fatty acids from lysophospholipids. *Proc. Natl. Acad. Sci. U.S.A.* 110, 8882–8887.
- Kanehisa, M., Furumichi, M., Sato, Y., Kawashima, M., Ishiguro-Watanabe, M., 2022. KEGG for taxonomy-based analysis of pathways and genomes. *Nucleic Acids Res.* 51, D587–D592 (2023).
- Kanehisa, M., Goto, S., 2000. KEGG: kyoto encyclopedia of genes and genomes. *Nucleic Acids Res.* 28, 27–30.
- Kaufmann, H., Mazur, X., Fussenegger, M., Bailey, J.E., 1999. Influence of low temperature on productivity, proteome and protein phosphorylation of CHO cells. *Biotechnol. Bioeng.* 63, 573–582.
- Keibler, M.A., Wasylenko, T.M., Kelleher, J.K., Iliopoulos, O., Vander Heiden, M.G., Stephanopoulos, G., 2016. Metabolic requirements for cancer cell proliferation. *Cancer Metabol.* 4.
- Khoo, S.H.G., Al-Rubeai, M., 2009. Detailed understanding of enhanced specific antibody productivity in NS0 myeloma cells. *Biotechnol. Bioeng.* 102, 188–199.
- Kiehl, T.R., Shen, D., Khattak, S.F., Li, Z.J., Sharfstein, S.T., 2011. Observations of cell size dynamics under osmotic stress. *Cytometry* 79A, 560–569.
- Klingenspor, M., Fromme, T., Hughes Jr., D.A., Manzke, L., Polyrneropoulos, E., Riemann, T., Trzcionka, M., Hirschberg, V., Jastroch, M., 2008. An ancient look at UCP1. *Biochim. Biophys. Acta Bioenerg.* 1777, 637–641.
- Knauf, J.A., Ouyang, B., Knudsen, E.S., Fukasawa, K., Babcock, G., Fagin, J.A., 2006. Oncogenic RAS induces accelerated transition through G(2)/M and promotes defects in the G(2) DNA damage and mitotic spindle checkpoints. *J. Biol. Chem.* 281, 3800–3809.
- Lambert, I.H., Pedersen, S.F., Poulsen, K.A., 2006. Activation of PLA(2) isoforms by cell swelling and ischaemia/hypoxia. *Acta Physiol.* 187, 75–85.
- Le, H., Kabbur, S., Pollastrini, L., Sun, Z.R., Mills, K., Johnson, K., Karypis, G., Hu, W.S., 2012. Multivariate analysis of cell culture bioprocess data-Lactate consumption as process indicator. *J. Biotechnol.* 162, 210–223.
- Lee, H.O., Davidson, J.M., Duronio, R.J., 2009. Endoreplication: polyploidy with purpose. *Gene Dev.* 23, 2461–2477.
- Liao, Y., Smyth, G.K., Shi, W., 2014. featureCounts: an efficient general purpose program for assigning sequence reads to genomic features. *Bioinformatics* 30, 923–930.
- Liu, Y., 2006. Fatty acid oxidation is a dominant bioenergetic pathway in prostate cancer. *Prostate Cancer Prostatic Dis.* 9, 230–234.
- Lobrich, M., Jeggo, P.A., 2007. The impact of a negligent G2/M checkpoint on genomic instability and cancer induction. *Nat. Rev. Cancer* 7, 861–869.
- Love, M.I., Huber, W., Anders, S., 2014. Moderated estimation of fold change and dispersion for RNA-seq data with DESeq2. *Genome Biol.* 15.
- Lukey, M.J., Katt, W.P., Cerione, R.A., 2017. Targeting amino acid metabolism for cancer therapy. *Drug Discov. Today* 22, 796–804.
- Luo, W.J., Brouwer, C., 2013. Pathview: an R/Bioconductor package for pathway-based data integration and visualization. *Bioinformatics* 29, 1830–1831.
- Malumbres, M., Barbacid, M., 2009. Cell cycle, CDKs and cancer: a changing paradigm. *Nat. Rev. Cancer* 9, 153–166.
- Marchant, R.J., Al-Fageeh, M.B., Underhill, M.F., Racher, A.J., Smales, C.M., 2008. Metabolic rates, growth phase, and mRNA levels influence cell-specific antibody production levels from in vitro-cultured mammalian cells at sub-physiological temperatures. *Mol. Biotechnol.* 39, 69–77.
- Marguerat, S., Baehler, J., 2012. Coordinating cell size. *Trends Genet.* 28, 560–565.
- Martinez, J.L., Meza, E., Petranovic, D., Nielson, J., 2016. The impact of respiration and oxidative stress response on recombinant α -amylase production by *Saccharomyces cerevisiae*. *Biotechnol. Bioeng.* 3, 205–210.
- Mcvey, D., Aronov, M., Rizzi, G., Cowan, A., Scott, C., Megill, J., Russell, R., Tirosh, B., 2016. CHO cells knocked out for TSC2 display an improved productivity of antibodies under fed batch conditions. *Biotechnol. Bioeng.* 113, 1942–1952.
- Meiri, S., Dayan, T., 2003. On the validity of Bergmann's rule. *J. Biogeogr.* 30, 331–351.
- Mistry, R.K., Kelsall, E., Sou, S.N., Barker, H., Jenness, M., Willis, K., Zurllo, F., Hatton, D., Gibson, S.J., 2021. A novel hydrogen peroxide evolved CHO host can improve the expression of difficult to express bispecific antibodies. *Biotechnol. Bioeng.* 118, 2326–2337.
- Moore, A., Mercer, J., Dutina, G., Donahue, C.J., Bauer, K.D., Mather, J.P., Etcheverry, T., Ryll, T., 1997. Effects of temperature shift on cell cycle, apoptosis and nucleotide pools in CHO cell batch cultures. *Cytotechnology* 23, 47–54.
- Nicholls, D., Cunningham, S., Wiesinger, H., 1986. Mechanisms of thermogenesis in BROWN adipose-tissue. *Biochem. Soc. Trans.* 14, 223–225.
- O'callaghan, P.M., Berthelot, M.E., Young, R.J., Graham, J.W.A., Racher, A.J., Aldana, D., 2015. Diversity in host clone performance within a Chinese hamster ovary cell line. *Biotechnol. Prog.* 31, 1187–1200.
- Padovan-Merhar, O., Nair, G.P., Biaisch, A.G., Mayer, A., Scarfone, S., Foley, S.W., Wu, A.R., Churchman, L.S., Singh, A., Raj, A., 2015. Single mammalian cells compensate for differences in cellular volume and DNA copy number through independent global transcriptional mechanisms. *Mol. Cell* 58, 339–352.
- Pan, X., Dalm, C., Wijffels, R.H., Martens, D.E., 2017. Metabolic characterization of a CHO cell size increase phase in fed-batch cultures. *Appl. Microbiol. Biotechnol.* 101, 8101–8113.
- Park, J.H., Noh, S.M., Woo, J.R., Kim, J.W., Lee, G.M., 2016. Valeric acid induces cell cycle arrest at G1 phase in CHO cell cultures and improves recombinant antibody productivity. *Biotechnol. J.* 11, 487–496.
- Park, J.U., Han, H.-J., Baik, J.Y., 2022. Energy metabolism in Chinese hamster ovary (CHO) cells: productivity and beyond. *Kor. J. Chem. Eng.* 39, 1097–1106.
- Prentice, H.L., Ehrenfels, B.N., Sisk, W.P., 2007. Improving performance of mammalian cells in fed-batch processes through "bioreactor evolution". *Biotechnol. Prog.* 23, 458–464.
- Puigserver, P., Wu, Z.D., Park, C.W., Graves, R., Wright, M., Spiegelman, B.M., 1998. A cold-inducible coactivator of nuclear receptors linked to adaptive thermogenesis. *Cell* 92, 829–839.
- Rial, E., Zardoya, R., 2009. Oxidative stress, thermogenesis and evolution of uncoupling proteins. *J. Biol.* 8, 58. Article No.: 58.
- Rieder, C.L., Cole, R.W., 2002. Cold-Shock and the mammalian cell cycle. *Cell Cycle* 1, 169–175.
- Sand, H., Cederlund, G., Danell, K., 1995. Geographical and latitudinal variation in growth-patterns and adult body-size of Swedish moose (ALCES-ALCES). *Oecologia* 102, 433–442.
- Sansregret, L., Swanton, C., 2017. The role of aneuploidy in cancer evolution. *Cold Spring Harbor Perspectives in Medicine* 7.
- Schellenberg, J., Nagraik, T., Wohlenberg, O.J., Ruhl, S., Bahnmann, J., Scheper, T., Solle, D., 2022. Stress-induced increase of monoclonal antibody production in CHO cells. *Eng. Life Sci.* 22, 427–436.
- Sinacore, M.S., Drapeau, D., Adamson, S.R., 2000. Adaptation of mammalian cells to growth in serum-free media. *Mol. Biotechnol.* 15, 249–257.
- Son, S., Tzur, A., Weng, Y., Jorgensen, P., Kim, J., Kirschner, M.W., Manalis, S.R., 2012. Direct observation of mammalian cell growth and size regulation. *Nat. Methods* 9, 910. -+.
- St-Pierre, J., Drori, S., Uldry, M., Silvaggi, J.M., Rhee, J., Jager, S., Handschin, C., Zheng, K.N., Lin, J.D., Yang, W.L., Simon, D.K., Bachoo, R., Spiegelman, B.M., 2006. Suppression of reactive oxygen species and neurodegeneration by the PGC-1 transcriptional coactivators. *Cell* 127, 397–408.
- Stier, A., Bize, P., Habold, C., Bouillaud, F., Masmelin, S., Criscuolo, F., 2014. Mitochondrial uncoupling prevents cold-induced oxidative stress: a case study using UCP1 knockout mice. *J. Exp. Biol.* 217, 624–630.
- Sunley, K., Tharmalingam, T., Butler, M., 2008. CHO cells adapted to hypothermic growth produce high yields of recombinant beta-interferon. *Biotechnol. Prog.* 24, 898–906.
- Tane, S., Chibazakura, T., 2009. Cyclin A overexpression induces chromosomal double-strand breaks in mammalian cells. *Cell Cycle* 8, 3900–3903.
- Templeton, N., Dean, J., Reddy, P., Young, J.D., 2013. Peak antibody production is associated with increased oxidative metabolism in an industrially relevant fed-batch CHO cell culture. *Biotechnol. Bioeng.* 110, 2013. -+.
- Thompson, S.L., Bakhom, S.F., Compton, D.A., 2010. Mechanisms of chromosomal instability. *Curr. Biol.* 20, R285–R295.
- Toleikis, A., Trumbeckaite, S., Liobikas, J., Pauziene, N., Kursvietiene, L., Kopustinskiene, D.M., 2020. Fatty acid oxidation and mitochondrial morphology changes as key modulators of the affinity for ADP in rat heart mitochondria. *Cells* 9.
- Toussaint, C., Henry, O., Durocher, Y., 2016. Metabolic engineering of CHO cells to alter lactate metabolism during fed-batch cultures. *J. Biotechnol.* 217, 122–131.

- Van Den Heuvel, S., Dyson, N.J., 2008. Conserved functions of the pRB and E2F families. *Nat. Rev. Mol. Cell Biol.* 9, 713–724.
- Wagstaff, J.L., Masterton, R.J., Povey, J.F., Smales, C.M., Howard, M.J., 2013. H-1 NMR spectroscopy profiling of metabolic reprogramming of Chinese hamster ovary cells upon a temperature shift during culture. *PLoS One* 8.
- Wang, S.Y., Huang, J.Z., Li, C.G., Zhao, L.Y., Wong, C.C., Zhai, J.N., Zhou, Y.F., Deng, W., Zeng, Y., Gao, S.S., Zhang, Y.Q., Wang, G.P., Guan, X.Y., Wei, H., Wong, S.H., He, H. S.H., Shay, J.W., Yu, J., 2020. MAP9 loss triggers chromosomal instability, initiates colorectal tumorigenesis, and is associated with poor survival of patients with colorectal cancer. *Clin. Cancer Res.* 26, 746–757.
- Weinguny, M., Klanert, G., Eisenhut, P., Jonsson, A., Ivansson, D., Lovgren, A., Borth, N., 2020. Directed evolution approach to enhance efficiency and speed of outgrowth during single cell subcloning of Chinese Hamster Ovary cells. *Comput. Struct. Biotechnol. J.* 18, 1320–1329.
- Xing, Z.Z., Kenty, B., Koyrakh, I., Borys, M., Pan, S.H., Li, Z.J., 2011. Optimizing amino acid composition of CHO cell culture media for a fusion protein production. *Process Biochem.* 46, 1423–1429.
- Xu, J., Tang, P., Yongky, A., Drew, B., Borys, M.C., Liu, S., Li, Z.J., 2019. Systematic development of temperature shift strategies for Chinese hamster ovary cells based on short duration cultures and kinetic modeling. *mAbs* 11, 191–204.
- Xu, L., Ma, X., Bagattin, A., Mueller, E., 2016. The transcriptional coactivator PGC1 alpha protects against hyperthermic stress via cooperation with the heat shock factor HSF1. *Cell Death Dis.* 7.
- Yoon, D.S., Wersto, R.P., Zhou, W.B., Chrest, F.J., Garrett, E.S., Kwon, T.K., Gabrielson, E., 2002. Variable levels of chromosomal instability and mitotic spindle checkpoint defects in breast cancer. *Am. J. Pathol.* 161, 391–397.
- Yoon, S.K., Hong, J.K., Choo, S.H., Song, J.Y., Park, H.W., Lee, G.M., 2006. Adaptation of Chinese hamster ovary cells to low culture temperature: cell growth and recombinant protein production. *J. Biotechnol.* 122, 463–472.
- Yoon, S.K., Hwang, S.O., Lee, G.M., 2004. Enhancing effect of low culture temperature on specific antibody productivity of recombinant Chinese hamster ovary cells: clonal variation. *Biotechnol. Prog.* 20, 1683–1688.
- Young, J.D., 2013. Metabolic flux rewiring in mammalian cell cultures. *Curr. Opin. Biotechnol.* 24, 1108–1115.
- Zhang, Z.Y., Yang, D., Xiang, J.W., Zhou, J.W., Cao, H., Che, Q.S., Bai, Y., Guo, J., Su, Z. Q., 2021. Non-shivering thermogenesis signalling regulation and potential therapeutic Applications of Brown adipose tissue. *Int. J. Biol. Sci.* 17, 2853–2870.
- Zhurinsky, J., Leonhard, K., Watt, S., Marguerat, S., Bahler, J., Nurse, P., 2010. A coordinated global control over cellular transcription. *Curr. Biol.* 20, 2010–2015.
- Zimmet, J., Ravid, K., 2000. Polyploidy: occurrence in nature, mechanisms, and significance for the megakaryocyte-platelet system. *Exp. Hematol.* 28, 3–16.